Molecular Therapy
Nucleic Acids
Original Article

A Novel Therapeutic Strategy for Cancer Using Phosphatidylserine Targeting Stearylamine-Bearing Cationic Liposomes

Manjarika De,[1,3] Sneha Ghosh,[1,3] Triparna Sen,[1,3,4] Md. Shadab,[1,5] Indranil Banerjee,[1,6] Santanu Basu,[2] and Nahid Ali[1]

[1]Infectious Diseases and Immunology Division, Indian Institute of Chemical Biology, Kolkata, West Bengal, India; [2]Department of Oncology, ESI Hospital, Kolkata, West Bengal, India

There is a pressing need for a ubiquitously expressed antigen or receptor on the tumor surface for successful mitigation of the deleterious side effects of chemotherapy. Phosphatidylserine (PS), normally constrained to the intracellular surface, is exposed on the external surface of tumors and most tumorigenic cell lines. Here we report that a novel PS-targeting liposome, phosphatidylcholine-stearylamine (PC-SA), induced apoptosis and showed potent anticancer effects as a single agent against a majority of cancer cell lines. We experimentally proved that this was due to a strong affinity for and direct interaction of these liposomes with PS. Complexation of the chemotherapeutic drugs doxorubicin and camptothecin in these vesicles demonstrated a manyfold enhancement in the efficacies of the drugs both *in vitro* and across three advanced tumor models without any signs of toxicity. Both free and drug-loaded liposomes were maximally confined to the tumor site with low tissue concentration. These data indicate that PC-SA is a unique and promising liposome that, alone and as a combination therapy, has anticancer potential across a wide range of cancer types.

INTRODUCTION

Chemotherapeutic regimes customarily available for cancer have problems of potential toxicities and detrimental side effects because of a lack of adequate tumor specificity.[1] Eventually, many patients become refractory to these treatments and ultimately succumb to their disease. The ultimate goal in current cancer therapy is to find a common marker for malignant cells that can be targeted by chemotherapeutic drugs without affecting nontransformed cells. Thus, the need for improvement in older therapies has led to much interest in the area of targeted chemotherapy for cancer.

The plasma membrane of normal cells is characterized by an asymmetric distribution of phospholipids on the membrane leaflets.[2] Phosphatidylserine (PS), the most abundant anionic phospholipid, is an exclusive constituent of the inner leaflet of the plasma membrane in most mammalian cells.[2–4] The internal positioning of PS is mediated by a membrane protein or ATP-dependent transporter, aminophospholipidtranslocase.[1,5] The asymmetry is lost because of reduced function of this translocase or oxidative stress in the tumor microenvironment or because of activation of the scramblase enzyme.[3,6] The loss of asymmetry, resulting in the exposure of PS on the surface, is a salient and universal feature of cancerous cells[6] and, specifically, tumor endothelial cells (ECs).[7] Exposure of PS on the surface of apoptotic cells, known as the death knell, is acknowledged for its importance as an apoptotic marker in all cells.[8] In this context, it is of interest to note that cancer cells display an elevated amount of PS on the outer surface[2,9–12] but without any sign of apoptosis.[2,4,6] Tumor cells (TCs) share a susceptibility to destruction by activated macrophages as a self-defense mechanism of the body.[4] Even though the mechanism of macrophages to distinguish between tumor and non-TCs still remains unknown, several lines of evidence suggest that PS is the recognition moiety for macrophages that potentiate killing of cancer cells. PS-specific activity being a natural mode of eradication of tumors has generated a lot of interest in exploiting PS as a target molecule.[1,4,9,13–18]

Since few anticancer drugs have the ability of self targeting,[19] entrapping the drug in a particular carrier, thereby delegating the tumor-targeting responsibility to the carrier, is an established strategy to achieve this goal.[17,20–26] We generated a novel cationic liposomal carrier, phosphatidylcholine-stearylamine (PC-SA), that strongly binds to PS exposed on the surface of cancer cells and tumors. We have selected SA-bearing cationic liposomes because of their PS specificity, which we had previously utilized for specifically targeting and killing

Received 26 October 2017; accepted 26 October 2017;
https://doi.org/10.1016/j.omtn.2017.10.019.

[3]These authors contributed equally to this work.

[4]Present address: Thoracic/Head & Neck Medical Oncology, Clinical Research Building, T8.3986, The University of Texas MD Anderson Cancer Center, Houston, TX, USA

[5]Present address: Department of Dermatology, School of Medicine, University of Alabama at Birmingham, Birmingham, AL, USA

[6]Present address: School of Medical Science & Technology, Indian Institute of Technology Kharagpur, Kharagpur 721302, India

Correspondence: Nahid Ali, Infectious Diseases and Immunology Division, Indian Institute of Chemical Biology, Kolkata, West Bengal, India.
E-mail: nali@iicb.res.in

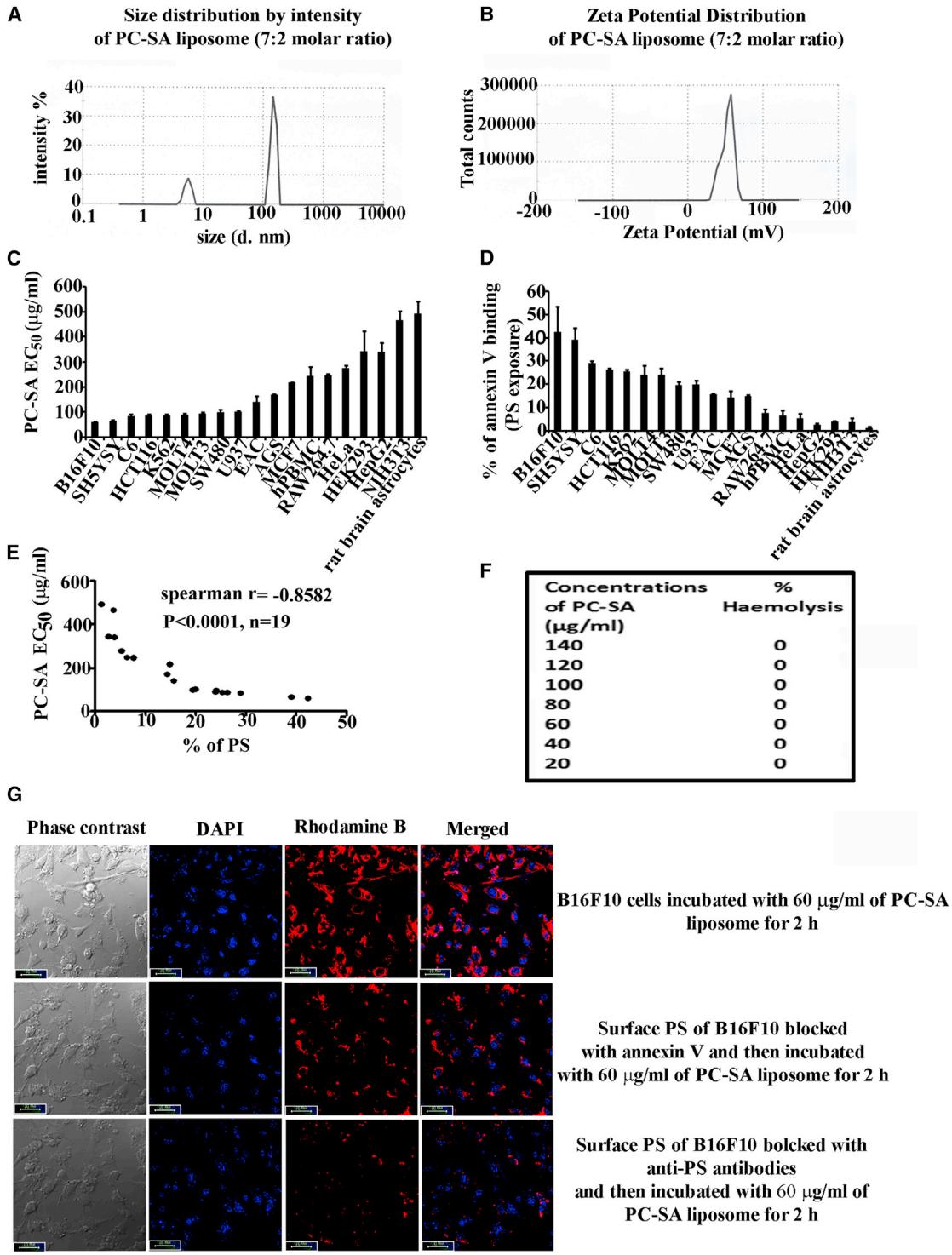

Figure 1. High PS Expression Predicts Sensitivity to PC-SA in Cancer Cell Lines

(A and B) Size distribution (A) and zeta potential (B) of PC-SA liposomes (7:2 molar ratio). (C) Viability of 19 cancerous and non-cancerous cells and cell lines after incubation with increasing concentrations of PC-SA for 2 hr. All data points represent the mean of at least three experiments, with error bars indicating the SEM. (D) PS exposure (percent of annexin V binding) of different cancer and non-cancer cells (flow cytometric analysis, 3 independent experiments for each cell line). (E) PS expression as assessed by flow

(legend continued on next page)

Leishmania parasites both *in vitro* and *in* vivo.[27] In the present study, for the first time, we report that SA-bearing liposomes kill cancer cells through specific and direct interaction with negatively charged surface-exposed PS. The target selectivity of PC-SA is proven through reversal of its anticancer activity when cells pretreated with annexin V and anti-PS antibodies bind to PS, and with anionic PC-PS liposomes, which bind to PC-SA vesicles. We could almost negate the possibility of interaction with other phospholipids, which, even if present, is negligible in amount compared with PS; hence, its effect can be nullified. PC-SA induced apoptosis in cancer cell lines and showed potent anticancer effects as a single agent. The effects of anticancer drugs like camptothecin and doxorubicin, entrapped in PC-SA liposomes on different cancer cell lines *in vitro* and across three mice preclinical models *in vivo*, clearly indicate the higher efficacy of the former compared with the free drugs. These observations therefore suggest that PC-SA vesicles elicit anticancer activity alone and also in combination with anticancer drugs and, thus, can prove its value as a significant addition to cancer therapy.

RESULTS

Particle Size, Morphology Analysis, and Zeta Potential of PC-SA Liposomes

A cationic liposome composed of PC (structure shown in Figure S1A) and SA (structure shown in Figure S1B) was prepared. PC-SA liposome showed a polydispersity index (PDI) of 0.2, indicating narrow distribution of particle sizes, and the hydrodynamic diameter, as measured by laser dynamic light scattering (DLS), was found to be 146 nm (Figure 1A). Additionally, AFM was performed to assess the morphology of the liposome. AFM analysis showed that the PC-SA liposome was spherical in structure, with intact morphology. It was also found that the particles are well apart from each other, and no significant aggregation was noticed (Figures S1C and S1D). Cross-section analysis of PC-SA liposomal particles showed a height image of 3.10–4.20 nm on a mica surface (Figure S1E), indicating that the particles are almost uniform. The zeta potential of PC-SA was found to be +52 mV (Figure 1B).

PC-SA Liposomes Selectively Target Cancer Cells by Directly Interacting with Surface-Exposed PS

PC-SA liposomes selectively killed the cancer cell lines B16F10, SH-SY5Y, SW480, HCT116, rat C6 glioma, MOLT-3, MOLT4, K-562, U-937, EAC, and AGS (half-maximal effective concentration [EC_{50}] = 65–170 μg/mL for 2 hr treatment) (Figure 1C). However, they showed weaker killing activity against non-cancerous cells and cancer cell lines, including HEK cells, NIH 3T3 cells, RAW 264.7 cells, healthy human peripheral blood mononuclear cells (PBMCs), MCF7 cells, HepG2 cells, HeLa cells, and rat brain astrocytes (EC_{50} = 218–480 μg/mL) (Figure 1C), with less surface-exposed PS (Figure 1D), indicating that PC-SA liposomes probably do not kill cells through an off-target mechanism. Notably, neutral PC-cholesterol (Chol) liposomes showed no activity against any of the cancer cell lines (Figure S2). Quantification of the amount of cell surface-exposed PS by us (Figure 1D) and others[9–11] showed that cancer cells have a higher amount of PS in comparison with normal cell lines and that the killing activity of PC-SA is strongly correlated with surface-exposed PS (Figure 1E). Red blood cells incubated with different concentrations of PC-SA liposomes showed no signs of hemolysis, suggesting a potential for their use as anticancer agent (Figure 1F).

Through confocal study, it was observed that PC-SA liposome could not interact with B16F10 cells in the presence of annexin V or anti-PS antibodies (Figure 1G), indicating that PC-SA liposomal activity is PS specific. In a cell viability assay, we blocked surface-exposed PS on the cancer cell lines B16F10, K562, rat C6 glioma, and U937 (Figures 2A–2D) with annexin V prior to addition of PC-SA liposomes. Interestingly, the killing activity of PC-SA liposomes was inhibited upon treatment. We got similar results when blocking PS of B16F10, K562, and U937 cells (Figures 2E–2G) with anti-PS antibodies prior to PC-SA treatment. Thus, it indicates that the killing is PS-mediated and that a high PS exposure status is a potential predictive marker for sensitivity to PC-SA liposomes and may have utility for patient stratification. The PS-specific affinity of PC-SA liposomes was further examined. PC-SA liposomes pre-incubated with PC-PS liposomes having a particle size distribution of 97.5 nm (hydrodynamic diameter as measured by DLS) (Figure S3A) with PDI of 0.28 and a zeta potential of −40 mV (Figure S3B) inhibited the killing activity of PC-SA liposomes on B16F10, K562, rat C6 glioma, and U937 cells. Moreover, the killing efficiency of PC-SA liposomes diminished with increasing concentrations of PC-PS liposomes (Figure 2H), indicating that the affinity of PS toward PC-SA liposomes is a critical factor that decides its activity. Here, the size of the liposome mixture (PC-SA and PC-PS) was observed to be 223 nm (hydrodynamic diameter as measured by DLS) (Figure S3C) with PDI of 0.342 and a zeta potential of +10 mV (Figure S3D).

When comparing PC-SA with other cationic liposomes (PC-dodecyltrimethylammonium bromide [DTAB], PC-dimethyldioctadecyl ammonium bromide [DDAB], and PC-N-[1-(2, 3-dioleoyloxy) propyl]-N,N,N-trimethylammonium chloride [DOTAP]), we found PC-SA to be more effective. Although PC-hexadecyltrimethylammonium bromide (CTAB) showed a killing activity similar to PC-SA, its activity was not PS-specific. PC-CTAB interacted with B16F10 cells even in the presence of annexin V or anti-PS antibodies (Figures S4A and S4B). Therefore, it is possible that PC-CTAB might be interacting with some other negatively charged phospholipids, which requires a thorough separate study.

cytometry and plotted against the corresponding PC-SA EC_{50} for each cell line (n = 19 lines). A significant correlation was observed between PS expression and PC-SA EC_{50} values (Spearman's rank correlation, $p < 0.0001$ by two-tailed t test). (F) Hemolytic assay in the presence of different concentrations of PC-SA (20–140 μg/mL). All concentrations show 0% hemolysis. (G) Interaction of Rhodamine B-PC-SA liposomes with B16F10 cancer cells in the presence or absence of annexin V or anti-PS antibodies, visualized under a confocal microscope (Leica TCS SP8, software LAS-X). Scale bars, 10 μm.

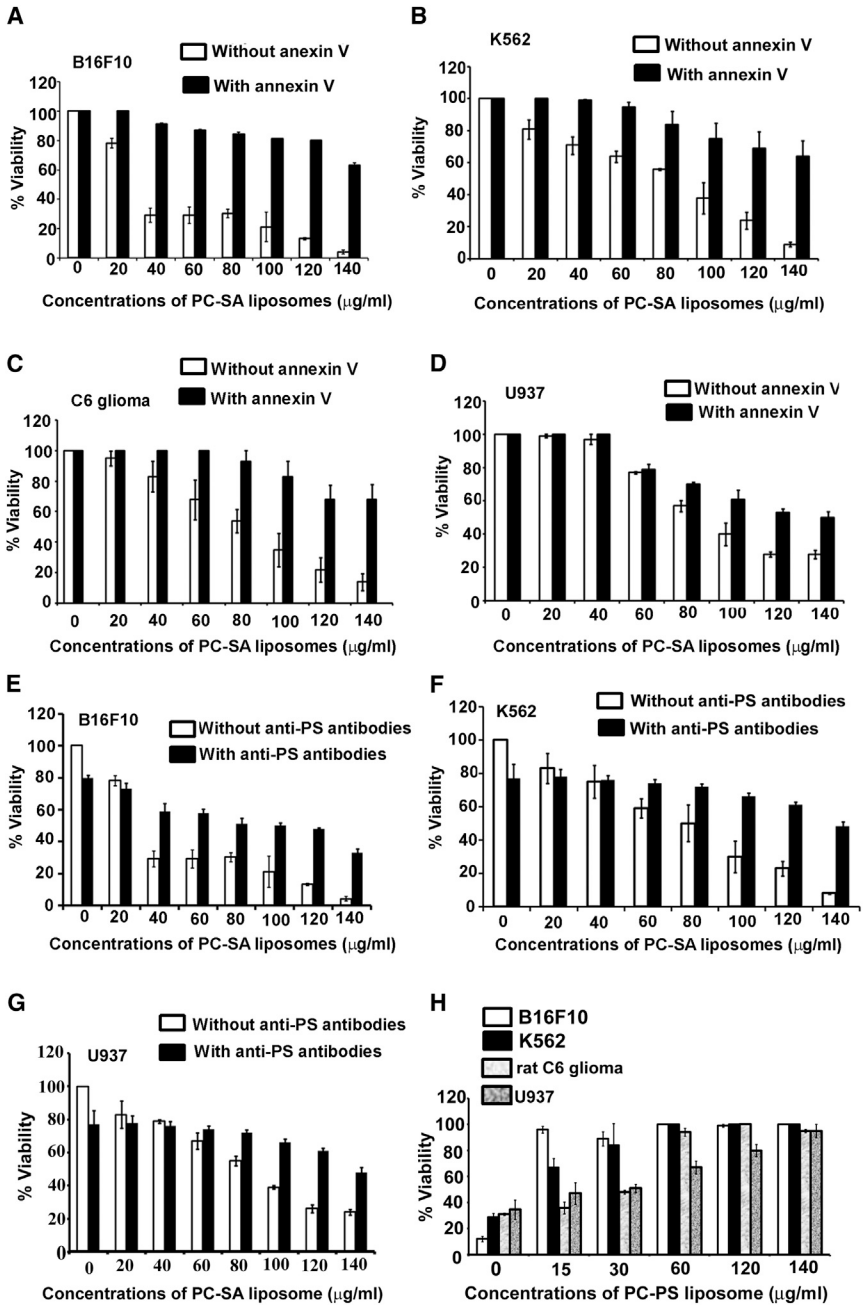

Figure 2. Role of PS Expressed on the Surface of Tumor Cells in Antitumor Activity of PC-SA Liposomes

(A–D) Treatment of annexin V-preincubated (A) B16F10, (B) K562, (C) rat C6 glioma, and (D) U937 cells with graded dose of PC-SA liposomes, showing a reversal in killing activity in comparison with cells that were not pretreated with annexin V. (E–G) Blocking of PC-SA liposomes by anti-PS antibodies. Treatment of anti-PS antibody-pre-incubated (E) B16F10, (F) K562, and (G) U937 cells with graded doses of PC-SA liposomes, showing a reversal in killing activity in comparison with cells that were not pre-treated with the antibodies. (H) Effect of the activity of a 7:2 molar ratio of PC-SA liposomes (120 μg/mL with respect to PC) after blocking it with different doses of PC-PS li-posomes (7:2). All data represent the mean of triplicate experiments, with error bars indicating the SEM.

Cellular Entrance Mechanism of PC-SA Liposomes

To clarify the cellular entrance mechanism of PC-SA liposomes, we measured cellular uptake by fluorescence-activated cell sorting analysis. We examined the effects of three inhibitors of cellular entrance pathways—the macropinocytosis (which is also known as actin-dependent endocytosis) inhibitor amiloride, the clathrin-mediated endocytosis inhibitor chlorpromazine, and the actin-dependent endocytosis inhibitor cytochalasin D—on cellular uptake of PC-SA-rhodamine 123 liposomes in B16F10 cells. In the presence of 500 μM amiloride, 31 μM chlorpromazine, and 500 μM cytochalasin D, there is approximately a 17%, 29% ($p < 0.001$), and 37% ($p < 0.001$) decrease in liposome uptake, respectively, compared with cells without the inhibitors. These results confirm that intracellular trafficking of PC-SA liposomes is mainly via endocytosis (Figures 3A and 3B). Other unidentified pathways may also be responsible for the liposomal uptake.

PC-SA Induces an Apoptotic Mode of Cell Death

Administration of PC-SA liposomes to the cancer cell lines B16F10, K562, and U937 rapidly (within 2 hr) induced key hallmarks of apoptosis. Treatment with PC-SA liposomes yielded a significant decrease in the mitochondrial red/green fluorescence intensity ratio in B16F10, K562, and U937 cell lines (because of loss of mitochondrial membrane potential, JC-1 remains in the monomer form, leading to a shift from red to green fluorescence) compared with untreated control cells (the high mitochondrial membrane potential of untreated healthy cells loaded with JC-1 allows formation of red fluorescent J aggregates),[28] suggesting that PC-SA treatment causes opening of mitochondrial permeability transition pores, resulting in mitochondrial membrane depolarization, whereas non-cancer cells (RAW 264.7) remained unaffected (Figure 3C). Treatment of B16F10, K562, and U937 cells with PC-SA (Figure 3D) resulted in reactive oxygen species (ROS) generation. The RAW264.7 cell line (Figure 3D) remained unaffected after treatment with the same concentrations of liposomes. PC-SA induced a distinct accumulation of sub-G0/G1 DNA (Figure 3E) and a further increase in the externalization of PS (Figure 3F), representing an increase in the population of apoptotic cells in the B16F10, K562, and U937 cell lines but not in the RAW264.7 cell line. Thus PC-SA caused

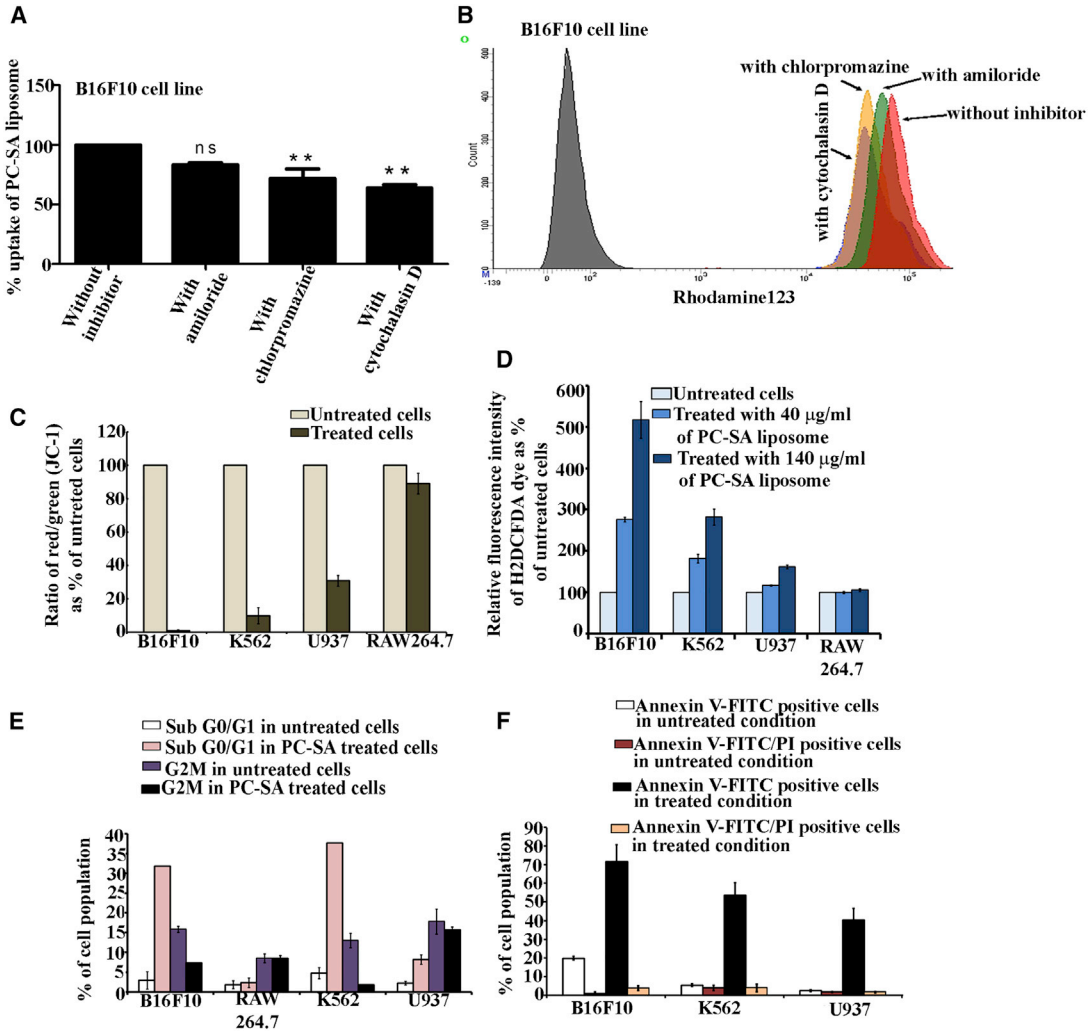

Figure 3. Cellular Entry of PC-SA Liposome and Its Role in Induction of Apoptosis

(A and B) Uptake of Rh123-PC-SA liposomes in B16F10 cells in the presence of inhibitors of endocytosis and macropinocytosis as determined by fluorescence-activated cell sorting (FACS). (A) PC-SA liposomes utilize clathrin and an actin-dependent endocytosis pathway mechanism for entry into target cells. (B) Shown are B16F10 cells without Rh123-PC-SA (grey peak), with Rh123-PC-SA (red peak), and with Rh123-PC-SA in the presence of cytochalasin D (blue peak), chlorpromazine (yellow), and amiloride (green). (C–F) PC-SA treatment for 2 hr after cellular entry induces multiple hallmarks of apoptosis in B16F10, K562, and U937 cells and has negligible effect on RAW264.7 cells. (C) Depolarization of the mitochondrial potential of cells treated with 140 μg/mL of PC-SA, stained with JC-1 and analyzed in a flow cytometer. The percentage of cells expressing green and red fluorescence is indicated. (D) To determine the effect of PC-SA liposomes on reactive oxygen species (ROS) generation, the B16F10, K562, U937, and RAW 264.7 cell lines were loaded with H2DCFDA after treatment with 40 and 140 μg/mL of PC-SA liposomes. The relative increase in fluorescence intensity of H2DCFDA as percent of untreated cells was measured. (E) Apoptosis (sub-G0/G1 accumulation and G2M) as assessed by FACS after treatment with 140 μg/mL of PC-SA liposomes. (F) Early and late apoptosis as determined by annexin V/PI staining by FACS after treatment with 140 μg/mL of PC-SA liposomes. All data represent the mean of triplicate experiments, with error bars indicating the SEM.

a significant cell death in cancer cells as compared to non-cancer cells. Moreover, cell killing mediated by PC-SA was caspase-, mitogen-activated protein kinase (MAPK)-, and phosphatidylinositol 3-kinase (PI3K)-dependent because their inhibitors specifically abrogated activity on K562 (Figures S5A, S5C, and S5E) and B16F10 (Figures S5B, S5D, and S5F) cells, whereas the AKT inhibitor could not inhibit the PC-SA killing activity in K562 (Figure S5G) and B16F10 (Figure S5H) cells because AKT is an anti-apoptotic marker.

To evaluate the role of MAPK pathways after PC-SA liposome treatment, whole-cell lysates were subjected to western blot using anti-phospho-ERK and anti-phospho-P38 antibodies. Phosphorylation of ERK increased significantly in the B16F10, K562, and U937 cell lines but not in the RAW264.7 cell line. Phosphorylation of P38 also increased in K562 and B16F10 cells (Figures 4B and 4C) but remained unchanged in the U937 (Figure 4A) and RAW264.7 (Figure 4D) cell lines. Significant increases in cleaved caspase-9, cleaved caspase-3, and cleaved

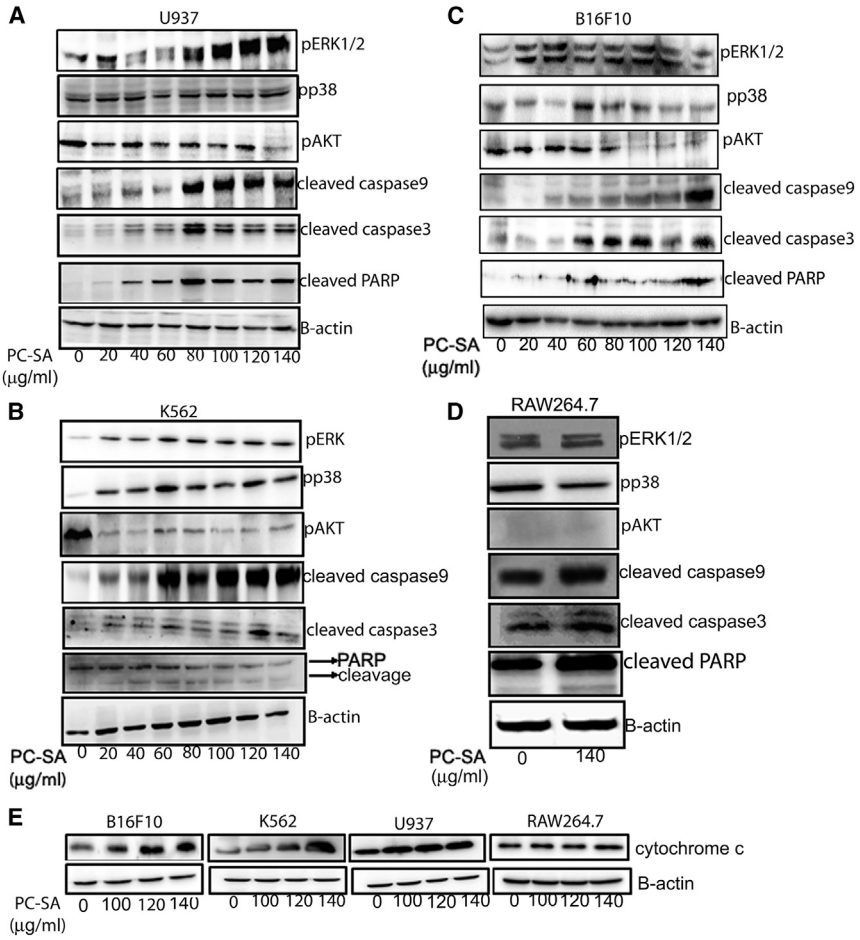

Figure 4. Immunoblot-Based Demonstration of the Involvement of p-ERK, pp38, p-AKT, Cleaved Caspase-9, Cleaved Caspase-3, Cleaved PARP, and Cytochrome *c* in 2-hr PC-SA-Treated Cells

(A–D) To check the involvement of signaling molecules in PC-SA-mediated apoptosis, (A) U937, (B) K562, (C) B16F10, and (D) RAW264.7 cells were treated with varying concentrations of PC-SA. The whole-cell lysates were subjected to western blot with anti-p-ERK, anti-pp38, anti-p-AKT, anti-cleaved caspase-3, anti-cleaved caspase-9, and anti-cleaved PARP antibodies. (E) Cytosolic fractions were subjected to western blot with anti-cytochrome *c* antibodies. Anti-β-actin antibodies were used to verify equal amounts of protein loading in each well.

PARP by PC-SA was observed in the U937, K562, and B16F10 (Figures 4A–4C) cell lines. It was observed that the total PARP (top band) in PC-SA-treated K562 cells decreased, but a significant increase in the cleavage of PARP (bottom band) was noted (Figure 4B). The RAW264.7 cell line (Figure 4D) remained unaffected. PC-SA liposomes downregulated the PI3K/Akt signaling pathway in U937, K562, and B16F10 (Figures 4A–4C) cells and caused no change in RAW264.7 cells (Figure 4D). Administration of PC-SA liposomes to B16F10, K562, and U937 cells rapidly induced cytochrome *c* release; RAW264.7 cells were least affected (Figure 4E). All of these findings indicate that, because PC-SA caused the most profound changes in the expression of apoptosis- and signaling-related proteins, the prominent apoptotic mode of cell death was observed in PC-SA-treated cancer cells. We also found that prolonged treatment (4 hr) of these cancer cells (U937) with PC-SA liposomes caused cell disruption with formation of large vacuoles and depletion of cytoplasmic material (Figure S6).

PC-SA Liposomes Enhance the Anticancer Effects of Camptothecin and Doxorubicin *In Vitro*

The EC_{50} values of free irinotecan hydrochloride (HCl) (a semisynthetic derivative of camptothecin [CPT]) were in the range of 800–5,000 μg/mL. In the case of entrapped CPT in PC-SA liposomes, the EC_{50} values were in the range of 2.5–3.5 μg/mL of CPT in combination with 50–70 μg/mL of PC-SA, which was significant compared with free irinotecan HCl ($p < 0.0001$) and free PC-SA ($p < 0.01$–0.0001) against B16F10, K562, U937, C6, MOLT4, and SW480 cells. For entrapped doxorubicin (DOX) in PC-SA liposomes, the EC_{50} values were in the range of 1.87–2.25 μg/mL of DOX in combination with 37–45 μg/mL of PC-SA, thus having a significantly ($p < 0.0001$) better killing effect than free DOX, which had EC_{50} values in the range of 500–800 μg /mL against B16F10, K562, U937, C6, MOLT4, and SW480 cells. It was also observed that DOX entrapped in PC-SA liposomes had a significantly better killing effect than free PC-SA ($p < 0.001$–0.0001) (Figure 5).

Acute Toxicity Investigations of PC-SA Liposomes

Acute toxicity investigations revealed no signs of mortality within 24 hr of administration of 220 mg of PC-SA liposomes. The animals were observed for another 15 days, and no apparent adverse effects (such as salivation, lacrimation, or skin rash) were seen. Only one of the four experimental animals died on day 10, and all other animals remained alive. The above results prove that 220 mg of PC-SA liposome did not reach LD50 value and could be safe for administration. Histopathological organ toxicity studies also revealed that there was no sign of toxicity in any of the vital organs compared with normal mice (Figure S7).

Preclinical Study to Determine the Effect of CPT-Entrapped PC-SA Liposomes on EAC Tumors

We chose 22 mg of PC-SA (which is 10 times less than the dose used for the acute toxicity study) for anticancer therapy alone or in combination with CPT against Ehrlich ascites carcinoma (EAC) induced in mice. On day 21, the body weights (wt) of EAC-injected control

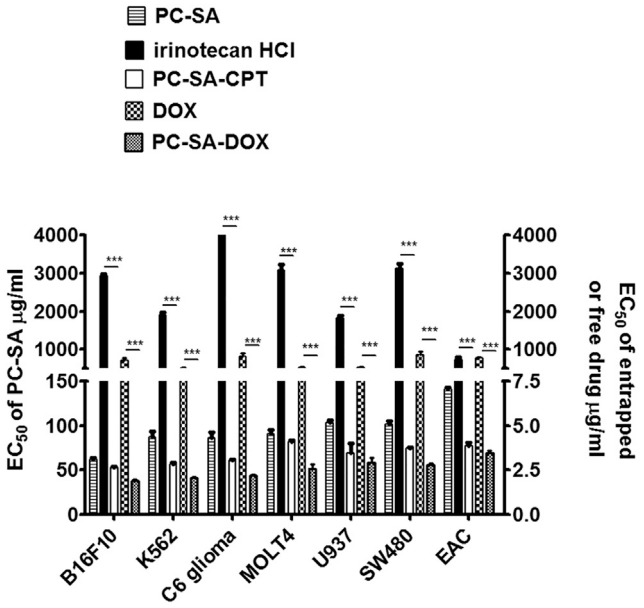

Figure 5. Effect of Anticancer Drugs Entrapped in PC-SA Liposomes on Cancer Cell Lines *In Vitro* following 2 hr Treatment

Camptothecin (CPT) at a molar ratio of 7 (PC):2 (SA):0.7 (CPT) and doxorubicin (DOX) at a molar ratio of 7 (PC):2 (SA):0.5 (DOX) showed 100% and 50% entrapment efficiency, respectively, in PC-SA liposomes. The EC_{50} values of DOX entrapped in PC-SA are 500-fold lower than that of free DOX ($p < 0.0001$) with respect to free DOX. Similarly, the EC_{50} values of CPT entrapped in PC-SA liposomes are 1,000-folds lower than that of free irinotecan HCl (a semisynthetic derivative of CPT) ($p < 0.0001$) with respect to free drug. The EC_{50} values of DOX or CPT entrapped in PC-SA liposomes with respect to PC are significantly lower than that of free liposomes ($p < 0.05$ to $p < 0.0001$). All data represent the mean of triplicate experiments, with error bars indicating the SEM.

mice increased because of accumulation of peritoneal fluid volume. Although EAC-injected mice treated on day 3 with a single injection of free PC-SA liposomes or irinotecan HCl showed a body wt increase, mice treated with CPT-entrapped PC-SA liposomes showed no such increase in comparison with control mice ($p < 0.01$) (Figure 6A; Figure S8). It was observed that the volume of peritoneal fluid (Figure 6B), packed cells (Figure 6C), and number of EAC cells (Figure 6D) decreased significantly when tumor-inoculated mice received CPT-entrapped PC-SA liposome treatment. Free PC-SA and free irinotecan HCl treatment showed a 37% reduction in peritoneal fluid volume in comparison with untreated control mice ($p < 0.01$) (Figure 6B). The survival of mice treated with PC-SA-CPT was prolonged to 53 days, which was significant compared with controls, ($p < 0.01$), PC-SA-treated ($p < 0.001$), and irinotecan HCl-treated ($p < 0.001$) mice (Figure 6E). There was no significant difference in the survival rate among the control, PC-SA-treated, and irinotecan HCl-treated groups. Estimation of serum SGPT, SGOT, creatinine, urea, and alkaline phosphatase for liver and kidney dysfunction (Figure 6G) and histopathological examinations of the tissues of the brain, lung, and heart (Figure S9) indicated that there were no detectable abnormalities between the normal, 22 mg PC-SA, 20 mg/kg of irinotecan HCl, and 20 mg/kg of CPT entrapped in 22 mg PC-SA drug injected intravenously (i.v.) normal Swiss albino mice, indicating no *in vivo* toxicity.

In Vivo Circulation Stability of Liposomal Drugs

Next, the plasma pharmacokinetics of CPT in PC-SA liposomes were compared with that of irinotecan HCl in normal mice. The persisting concentration of CPT in PC-SA liposomes in plasma, 1 and 2 hr after injection, was significantly higher than that of irinotecan HCl. The area under curve (AUC) values of CPT in PC-SA and irinotecan HCl were 182 and 94 μg·h/mL, respectively. The $T_{1/2}$ values of CPT in PC-SA and irinotecan HCl were 4.8 and 1.2 hr, respectively. The C_{max} values of CPT in PC-SA and irinotecan HCl were 24 μg/mL and 17 μg/mL, respectively. Thus, liposomal CPT showed about 2-fold higher AUC, 4-fold higher $T_{1/2}$, and 1.4-fold higher C_{max} values than irinotecan HCl (Figure 6H). It was also observed that a fluorescent anticancer drug, DOX (the uptake of this drug is detected through confocal microscopy), in its free form is easily taken up by *in vivo* macrophages (mononuclear phagocytic cells) at a very early time point, whereas DOX entrapped in PC-SA liposomes is taken up at a much later time point when injected i.v. in normal mice, indicating that PC-SA liposomes enhance the circulatory half-lives of anticancer drugs (data not shown).

Biodistribution of CPT Entrapped in PC-SA Liposomes in Mice Bearing EAC

The concentrations of CPT in PC-SA liposomes and irinotecan HCl present in different organs and peritoneal fluid in EAC-bearing mice are plotted in Figures 6I and 6J. 2 hr after administration of formulations, CPT from the entrapped liposome and irinotecan HCl were distributed to all major organs, including EAC peritoneal fluid. CPT concentrations increased in all organs and peritoneal fluid at 4 hr compared with those detected at the 2 hr time point. The 4-hr CPT concentration detected in animals treated with 20 mg/kg body wt entrapped in 22 mg PC-SA was greatest in EAC peritoneal fluid (16.4 μg/g), followed by the kidney (6.5 μg/g), liver (6.4 μg/g), lungs (5.9 μg/g), spleen (5.9 μg/g), heart (5.3 μg/g), and brain (1.7 μg/g). Thus, significant and specific uptake of PC-SA-CPT in EAC peritoneal fluid resulted in a higher distribution of CPT in the peritoneal cavity than in any other organs. The CPT levels in all organs, including peritoneal fluid, at 7 hr decreased relatively to the levels detected at the 4-h time point (Figure 6I). The 4-h irinotecan HCl concentrations detected in animals treated with 20 mg/kg body wt were 8.6 μg/g in the spleen, 6.4 μg/g in the liver, 6.5 μg/g in the kidneys, 6.2 μg/g in the heart, 5.7 μg/g in the brain, 3.6 μg/g in EAC peritoneal fluid, and 2.5 μg/g in the lungs (Figure 6J). Hence, the studies presented here indicate that administration of CPT entrapped in PC-SA liposomes leads to enhanced distribution to EAC peritoneal fluid; i.e., 8-fold higher compared with irinotecan alone.

Preclinical Study to Validate that DOX and CPT Entrapped in PC-SA Liposomes Reduces the B16F10 Tumor Burden

After successful remediation in Swiss albino mice, we next moved to advanced B16F10 tumor models. One of minimal disease and

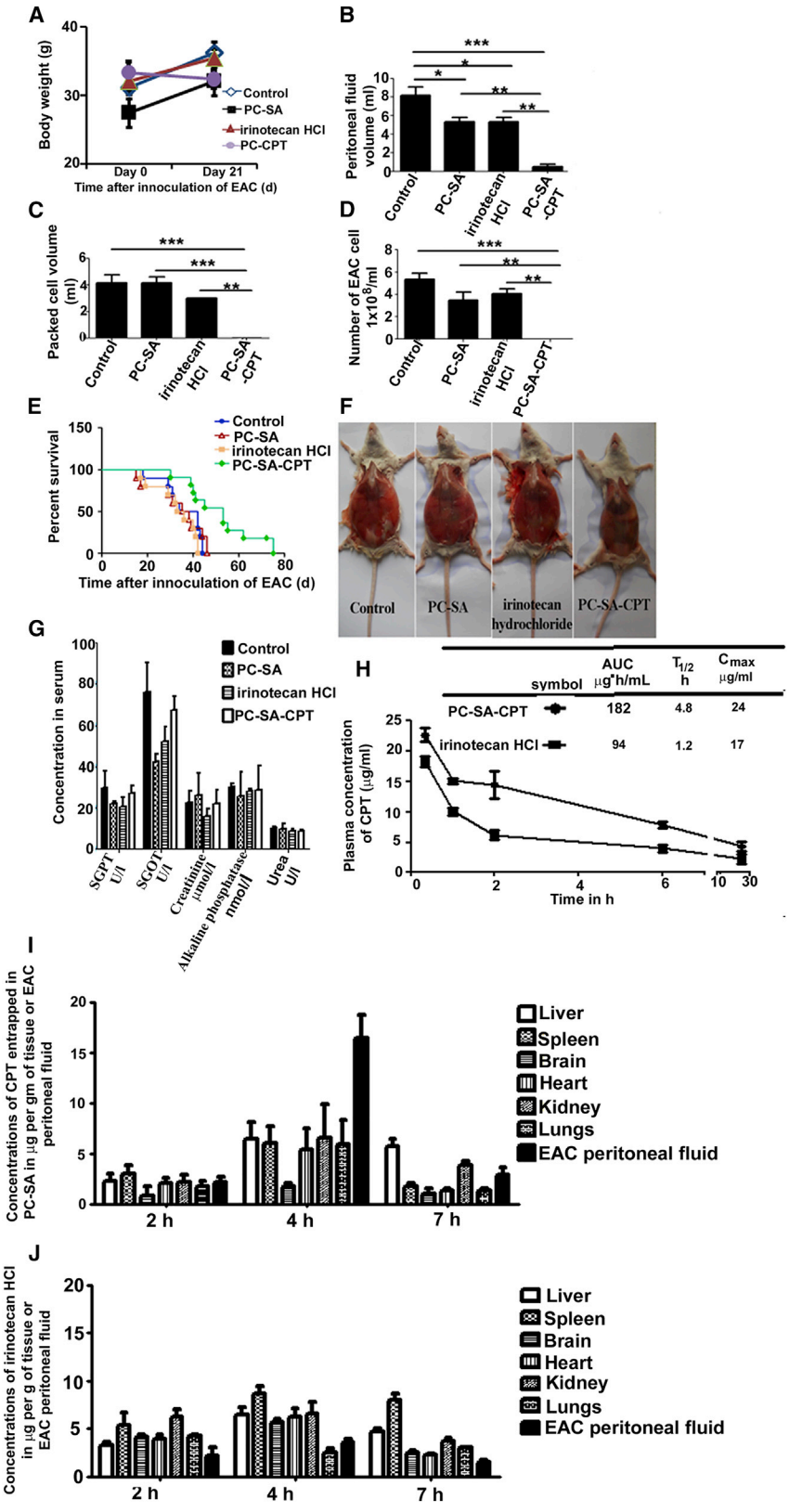

Figure 6. PC-SA Liposomes Inhibit EAC Growth as a Single Agent and in Combination with Anticancer Drugs

22 mg of PC-SA liposomes, 20 mg/kg of irinotecan HCl (a semisynthetic derivative of CPT), and 20 mg/kg of CPT entrapped in 22 mg of PC-SA liposomes were administered on day 2 intravenously into EAC-bearing Swiss albino mice. (A) Body weights were taken. (B–D) Mice were sacrificed on day 21, and (B) peritoneal fluid volume, (C) packed cell volume, and (D) the number of EAC cells were measured. (E) The cumulative survival curve (Kaplan-Meier survival plot) of another set of mice was plotted against time after inoculation of EAC in days. (F) Images of mice. (G) No significant toxic effects of PC-SA-CPT, PC-SA, and irinotecan HCl were observed in any of the organs of normal Swiss albino mice. (H) Plasma concentration time curves of CPT (20 mg/kg) in PC-SA and irinotecan HCl (20 mg/kg) following i.v. injection in normal Swiss albino mice. Each value represents the mean ± SD (n = 3). (I and J) Mean CPT concentration-time profiles in organs and the peritoneal cavity after single intravenous administration of CPT (20 mg/kg) entrapped in 22 mg of PC-SA (I) or 20 mg/kg irinotecan HCl (J) in EAC-bearing Swiss albino mice. Data represent mean ± SE for three animals per group performed in triplicate.

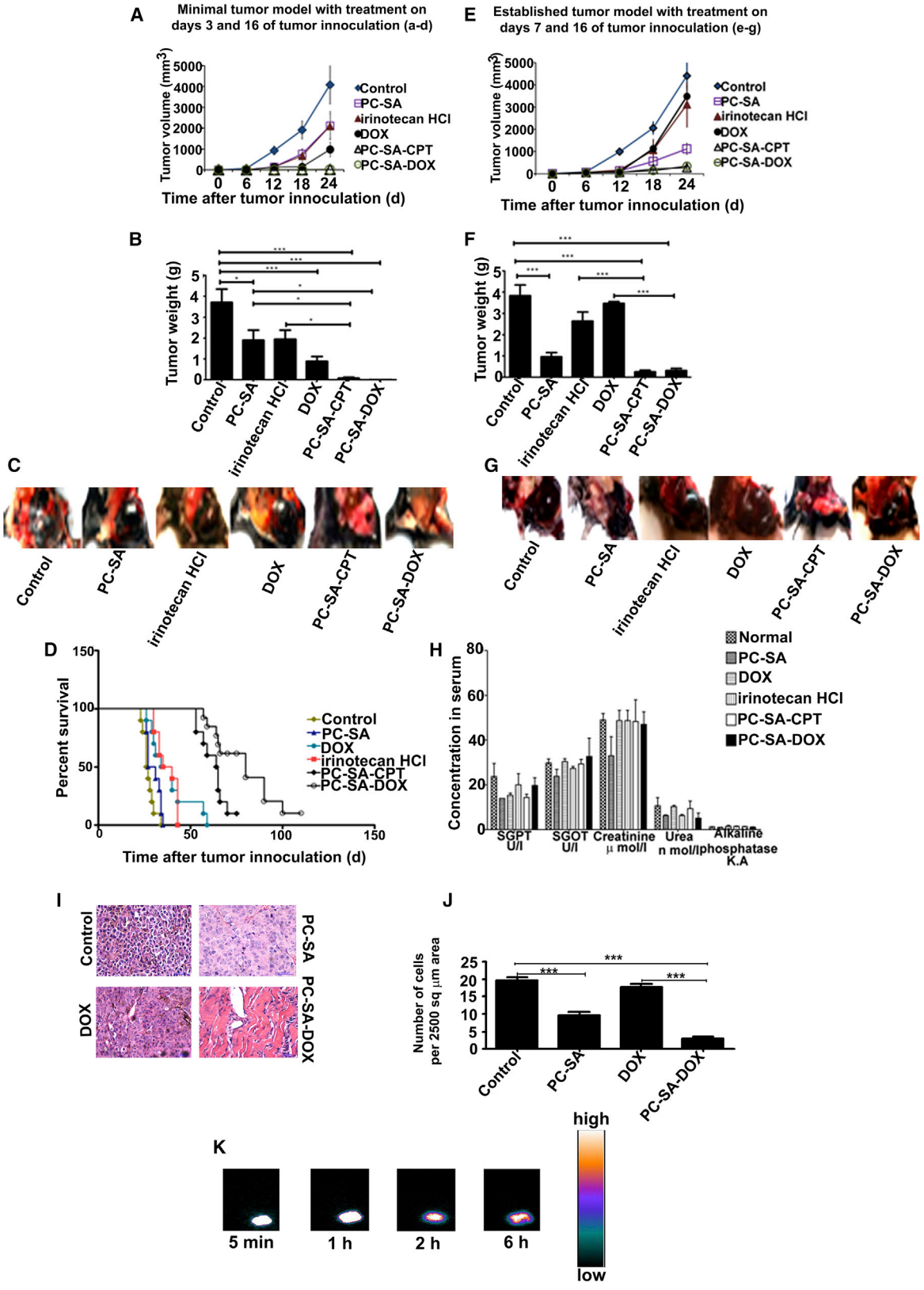

(legend on next page)

one of large established tumors were used to test the antitumor effect of liposomes as combination therapy with DOX and CPT on B16F10 tumors in C57BL6. Double injections of PC-SA liposomes in combination with CPT or DOX on days 3 and 16 of tumor induction completely reduced B16F10 tumors. Remarkably, in all mice so treated, there was a complete absence of tumors, excepting one, in which negligible tumor growth was detected. Tumor volumes (Figure 7A) and weights (Figure 7B) were below the level of detection in all animals treated with PC-SA-DOX (tumor growth inhibition [TGI] = 99%, $p < 0.0001$) and PC-SA-CPT (TGI = 99%, $p < 0.0001$). The tumor volume also decreased significantly following treatment with double injection of free DOX (TGI = 77%, $p < 0.0001$) or irinotecan HCl (TGI = 48%, $p < 0.01$) compared with untreated, tumor-bearing controls. Double injection of drug-free PC-SA liposomes also reduced the tumors significant (TGI = 48%, $p < 0.01$) (Figure 7C). Interestingly delivery of DOX entrapped in PC-SA and CPT entrapped in PC-SA resulted in further extension of the lifespan, with median survival of 80 and 64 days, respectively, relative to the groups treated with free DOX, free irinotecan HCl, free PC-SA, and controls ($p < 0.0001$) (Figure 7D).

In the large established model, when mice were treated on days 7 and 16 of tumor induction—i.e., when tumors were palpable (65–75 mm^3 in volume), tumor growth (Figures 7E and 7F) was suppressed by 90% ($p < 0.0001$) in the group receiving PC-SA-DOX and PC-SA-CPT and by 74% ($p < 0.001$) in the group receiving only PC-SA liposome (Figure 7G). Estimation of serum SGPT, SGOT, creatinine, urea, and alkaline phosphatase for liver and kidney dysfunction 15 days after injection of PC-SA, DOX, PC-SA-DOX, irinotecan HCl, and PC-SA-CPT subcutaneously (s.c.) in C57/BL6 (Figure 7H) demonstrated normal levels, indicating no *in vivo* toxicity.

Tumor Histopathology Analysis

Tumor tissues were fixed and stained. H&E staining of the tumor sections showed the active growth of TCs, with obvious nuclear division and rich vessels in control and doxorubicin-treated tumors. TCs grew slowly in tissue sections of PC-SA-treated mice. The tumor section of mice treated with PC-SA-DOX showed significantly fewer TCs, and a larger portion of the section showed the formation of matrix (Figure 7I). The numbers of TCs found in the tumor tissue section per 2,500 μm^2 area was also much reduced in the PC-SA-DOX- and PC-SA-treated groups compared with that in the DOX-treated group and untreated control group (Figure 7J).

Scintigraphy of ^{99m}Tc-PC-SA liposomes in B16F10 Tumor-Bearing Mice

More than 95% (97.44% ± 0.24%, n = 4) of ^{99m}Tc was found to label PC-SA liposomes, as calculated from the labeling efficiency equation. The resulting complex of ^{99m}Tc-PC-SA was found to be quite stable up to 6 hr (labeling efficiency was maintained ~90%) (Table S1).

Figure 7K illustrates whole-body images of a B16F10 tumor-bearing mouse 5 min, 1 hr, 2 hr, and 6 hr after s.c. administration of ^{99m}Tc-PC-SA liposomes. ^{99m}Tc -PC-SA liposomes administered by s.c. injection experienced rapid tumor uptake (whole tumor visualized 5 min after s.c. injection of ^{99m}Tc-PC-SA liposomes). We observed prolonged retention of ^{99m}Tc liposomes at the tumor site (i.e., up to 6 hr in this experimental setting), which could be due to specific interaction of PC-SA liposomes with PS exposed on the surface of the solid tumor. This suggests that s.c. administration of PC-SA liposomes at the tumor site facilitates significant uptake, resulting in effective tumor therapy followed by tumor regression.

Uptake of PC-SA-DOX and Free DOX by B16F10 TCs

Confocal microscopic analysis of B16F10 TCs isolated at different time points from B16F10 solid tumors of C57Bl6 mice injected with free DOX and liposomal DOX revealed that, at the 2-hr time point, expression of DOX is more intense in TCs of mice injected with PC-SA-DOX in comparison with that of mice injected with free DOX. At the 4-hr and 8-hr time points, the intensity of DOX expression increased in the TC nuclei of mice injected with PC-SA-DOX. On the contrary, expression of DOX in TCs was very low in mice injected with the same dose of free DOX, indicating rapid elimination of free DOX from the tumor site. This study further supports prolonged retention of PC-SA-DOX in TCs (i.e., up to 8 hr in this experimental setting) (Figure S10). This observation also suggests that PC-SA liposomes may be an effective means of achieving sustained intratumoral release of entrapped drugs.

Figure 7. PC-SA Liposomes Inhibit B16F10 Tumor Growth as a Single Agent and in Combination with Anticancer Drugs

(A–G) On days 3 and 16 (A–D) and on days 7 and 16 (E–G), tumor induced C57BL6 mice were administered, s.c. at the tumor site, PC-SA liposomes alone, 8.4 mg/kg of free irinotecan HCl, 2.8 mg/kg of free DOX, 8.4 mg/kg of CPT entrapped in 60 mg/kg of PC-SA liposomes, and 2.8 mg/kg of DOX entrapped in 60 mg/kg of PC-SA liposomes. Mice injected with B16F10 cells and left untreated served as a control. Tumor response was observed every week (A and E), and mice were sacrificed and photographed on day 24 of tumor induction (C and G) to measure the tumor weight (B and F). Tumor volumes and weights measured for PC-SA, PC-SA-DOX, and PC-SA-CPT groups on day 24 were significantly lower compared with untreated tumor-induced groups. PC-SA-CPT and PC-SA-DOX showed complete clearance of tumor when the treatment was started at an early time point (i.e., on days 3 and 16), whereas, when the treatment was started at a later time point (i.e., on days 7 and16), there was a 90% reduction in tumor growth. (D) Kaplan-Meier survival curves show that early treatment with PC-SA-DOX and PC-SA-CPT increases survival in mice bearing tumors. (H) No significant elevation was observed in any of the toxicity markers compared with the controls (see text for details). (I) H&E staining of tumor tissue sections from C57BL6 mice induced with B16F10 tumor and mice treated on days 7 and 16 of tumor induction with 60 mg/kg of PC-SA, 2.8 mg/kg of DOX, and 2.8 mg/kg of DOX entrapped in 60 mg/kg of PC-SA (magnification ×40). (J) Number of tumor cells per 2,500 μm^2 field area from the images of the above H&E-stained tissue sections (n = 3 fields). (K) Gamma scintigraphic images of a B16F10 tumor-bearing C57BL6 mouse after subcutaneous injection of ^{99m}Tc-PC-SA liposomes taken at 5 min, 1 hr, 2 hr, and 6 hr post-injection demonstrate uptake and retention of the liposome at the tumor site. Data represent mean ± SE for three animals per group performed in triplicate.

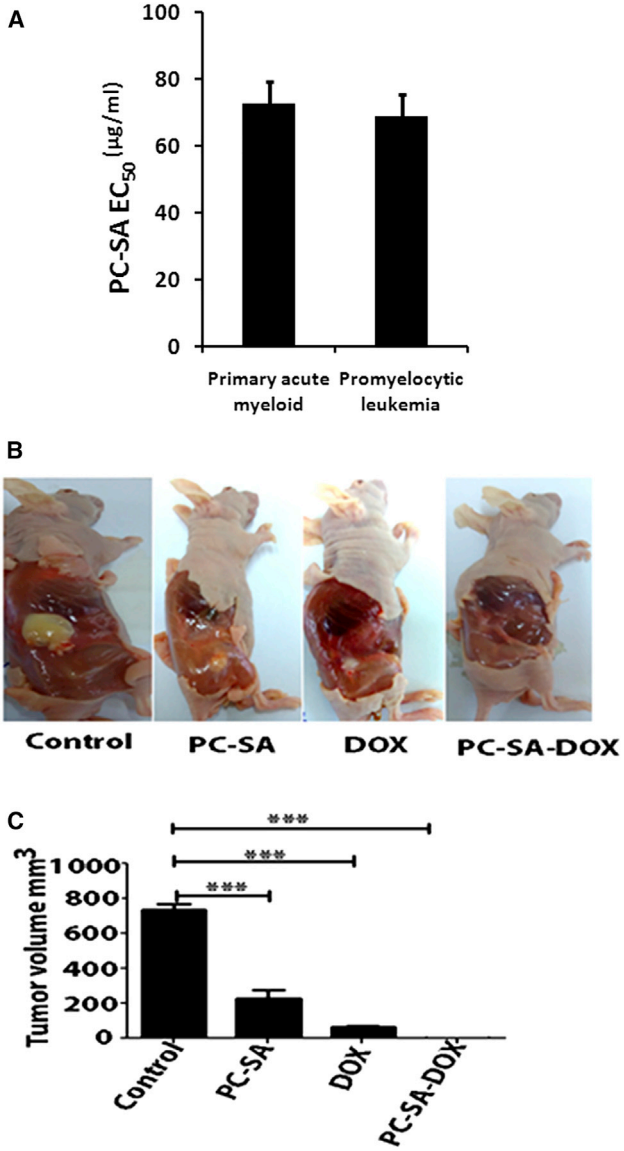

Figure 8. Validation of PC-SA Liposomes on PBMCs of Leukemia Patients and K562 Xenograft Model in Nude Mice

(A) PBMCs from 3 primary acute myeloid and promyelocytic leukemia patients were cultured in medium with graded doses of PC-SA liposomes for 2 hr, and cell viability was determined by MTT. (B and C) K562 cells embedded in Matrigel were staged in nude mice. On days 7 and 16, mice were administered 60 mg/kg of PC-SA liposomes alone, 2.8 mg/kg of free DOX, and 2.8 mg/kg of DOX entrapped in 60 mg/kg of PC-SA liposomes subcutaneously and sacrificed (B) on day 24 to measure the tumor growth (C). Data represent mean ± SE for three animals per group performed in duplicate.

In Vivo PC-SA and PC-SA-DOX Therapy Inhibited Tumor Vasculature in B16F10 Tumor-Induced Mice

The expression and distribution of CD31, which is a well-known angiogenic or EC marker used in vascular tumors,[29,30] were investigated by immunohistochemistry. A decrease in the expression of CD31 was observed in tumor tissue sections of PC-SA-treated groups in comparison with untreated control and DOX-treated mice. It was observed that expression of CD31 on PC-SA-DOX-treated tumors was absent and similar to that of normal tissue (Figure S11). This indicates that PC-SA and PC-SA-DOX had an effect on the decrease in formation of tumor microvasculature, thus inhibiting angiogenesis, which could be due to high expression of PS on the tumor vasculature.

Uptake of PC-SA Liposomes by Tumor Cells Is Not Limited by ECs

ECs that were CD31-positive (CD31 is an EC marker) and TCs isolated from B16F10 tumor-induced C57BL6 mice injected with PC-SA-FITC liposomes were visualized under a confocal microscope. It was found that PC-SA liposomes (green fluorescence) were taken up by the TCs even in the presence of ECs (red fluorescence). Entry of the liposome was also observed in some of the ECs, which could be due to the expression of PS on these cells (Figure S12). This observation shows that intratumoral uptake of liposomes is not inhibited by ECs.

Preclinical Validation of PC-SA Liposomes on Leukemic Patient Samples and Authentication of the Potent Antitumor Efficacy of DOX Entrapped in PC-SA Liposomes on K562 Xenograft Tumor Growth in Nude Mice

PC-SA liposomes reduced the viability of primary acute myeloid leukemia (AML) (EC_{50} = 72.5 μg/mL ± 6.6) and acute promyelocytic (EC_{50} = 69 μg/mL ± 3.9) leukemic patient cells in a dose-dependent manner (Figure 8A). Administration of PC-SA ($p < 0.0001$) and free DOX ($p < 0.0001$) in an advanced K562 xenograft model in nude mice reduced tumor growth significantly compared with untreated mice. Interestingly, delivery of DOX entrapped in PC-SA resulted in complete remission of tumor volume ($p < 0.0001$) (Figures 8B and 8C).

DISCUSSION

PS, an anionic phospholipid tightly segregated to the internal surface of the plasma membrane of resting mammalian cells, has been reported to be exposed on vascular ECs in tumors.[11,16,31,32] This externalized anionic phospholipid on hitherto viable cells has been identified as one of the most specific markers of tumor vasculature.[3,4,7,33,34] Because PS is also expressed constitutively on some TCs,[4] it prompted us to test the anticancer effect of PC-SA liposomes, a novel carrier having strong affinity for PS. In this study, we unravel a distinguishing tumoricidal activity of PC-SA liposomes *in vitro* and *in vivo*. Entrapment of established drugs, DOX and CPT, in these vesicles enhanced their efficacies for almost complete remission. The anticancer activity of these liposomes involves specific interaction of PC-SA with induction of apoptosis in PS-overexpressing cells.

In this study, cationic liposomes of reproducible size (146 nm) and charge (+52 mV) composed of PC and SA were utilized to target PS exposed on TCs. PC-SA as a monotherapy demonstrates 50%–96% killing activity on multiple cancer cell lines (patent application number WO2015040636A1). Several lines of evidence are available regarding cationic liposomes being utilized for selective delivery of

anticancer drugs to the tumor vasculature,[22,25,35] which results in improved therapeutic efficacy and longer survival. However, none of these studies show a killing activity of the cationic liposome alone, and they also fail to elucidate a detailed mechanism of the enhanced antitumor efficacy. The activity of PC-SA vesicles directly correlates with the extent of PS exposure, emphasizing the novel, selective, and specific cytotoxic effect of PC-SA on cancer cells with a higher PS percentage. Some cancer cell lines, like MCF7 and HepG2, and non-cancer cells, like HEK293 cells, human PBMCs (hPBMCs), etc., which have a lesser amount of surface-exposed PS, require a much higher dose to kill them. Thus, at the therapeutic dose, normal cells are expected to remain almost unaffected. This unexpected activity of the liposome alone prompted us to test the mechanism behind it. Interestingly, we found that, when we blocked PS on cancer cells with its binding protein Annexin V and treated it with a graded dose of fluorescently tagged PC-SA, the liposome could not enter the cell, and the killing activity was reversed. When cells pretreated with PS-specific antibodies, which are known to interact with PS and induce killing activity,[15] were treated with PC-SA even though a certain killing activity because of PS antibodies was seen, it notably reversed the TC inhibition of PC-SA. We could therefore say that cross-interaction of PC-SA with other anionic phospholipids, if present, is negligible. These observations therefore ascertain that PS plays a direct role in PC-SA-induced cell death. Following interaction with PC-SA, an increase in PS exposure on the external surface is observed, probably caused by ROS generation,[7,15] ameliorating the apoptotic activity of these liposomes. Notably, we found that the liposome enters the cell via endocytosis and that malignant cell death caused by PC-SA is associated with activation of the MAPKs (such as phosphorylated p38 and phosphorylated ERK 1/2), downregulation of AKT, and cell cycle arrest at sub-G0/G1 level specifically in malignant cancer cells. Interestingly, a similar PS targeting ability and anticancer activity of drug-free nanoparticles modified with zinc(II)-dipicoylamine[18] or Saposin C have been reported.[14,17]

Interestingly, when we compared the killing activity of the liposome with that of free drugs like DOX and CPT, liposomes alone showed much better anticancer activity. In this study we therefore sought to ascertain whether the anticancer efficacy of PC-SA enhances or acts synergistically when combined with DOX and CPT. Upon entrapment of DOX and CPT into PC-SA vesicles, we found synergistic enhancement of the efficacy of these drugs. Earlier reports of other liposomal DOX and CPT lend support to our view.[32,36–38] However, unlike here, these studies do not show a significant difference in the anticancer efficacy of the free versus encapsulated drug. This may be credited to the anticancer potential of PC-SA as a single agent, which results in the synergistic effect of these drugs.

There are many previous reports that show that liposomes enhance the efficacy of the drug and also aid in reducing the toxicity of the drugs,[21] which further results in altering the pharmacokinetics of the drug. Liposomes in the size range of 100–200 nm with higher zeta permeability increase the retention and cellular uptake of the drug.[39,40] Incorporation of SA in the vesicles suppresses the clearance of liposomes by Kupffer cells,[41] and a longer acyl chain (C-18) can enhance the plasma concentration of the drug.[42] We show in this study that PC-SA liposomes successfully entrap drugs like DOX and CPT with about 50% and 100% efficiency, respectively, and have a hydrodynamic diameter of about 150 nm, which leads to slow release of the drugs and prolonged circulation in the plasma. The pharmacokinetic parameters of free irinotecan and liposome-entrapped CPT showed a significant increase in $T_{1/2}$ to almost 4 hr in the case of CPT entrapped in liposomes. Biodistribution studies confirmed the pharmacokinetic values. In particular, by observing the distribution of irinotecan and liposomal CPT in different organs of mice, it was found that the entrapped drug was present in maximum up to 4 hr and was mostly confined to the tumor. In contrast, the free irinotecan uptake in peritoneal fluid was considerably low. Notably, scintigraphic images of mice s.c. injected with PC-SA showed that the liposomes were confined specifically to the tumor site. Subcutaneous injections are advantageous because they result in maximum uptake by the tumor and also almost negligible tissue distribution.[43] In the case of PC-SA, this could also be due to strong interaction with PS on the surface of the tumor, resulting in complete uptake by the tumor. Striking results from the study of expression of the CD31 marker sheds light on the fact that PC-SA alone and along with drug aids in the reduction of tumor vasculature. Thus, this formulation has potential anticancer as well as antivascular effects.

The therapeutic efficacy of the formulation was tested in several mouse models. Mouse models of EAC-bearing Swiss albino mice, B16F10-induced C57BL/6 mice, and K562-induced nude mice following tumor volume and wt, body wt, and survival are clear indicators of the positive effect of the formulation on therapeutic responses. Interestingly a single dose of PC-SA-entrapped CPT could completely cure EAC-bearing Swiss albino mice at a dose at which its free form could not induce any significant tumor inhibition. Here, in the minimal tumor model of B16F10, we show almost complete tumor remission, with the mice surviving up to 70–90 days after treatment with low doses of CPT and DOX and almost completely devoid of any signs of toxicity and tumor relapse. It is interesting to note that, in both the minor and large established tumor models, PC-SA has significant killing activity, correlating with the *in vitro* efficacy. The toxicity of SA-based liposomes is a major concern. Hemolytic assays by us and others,[44] toxicity parameter study of the kidney and liver, and histopathological analysis after i.v. administration of PC-SA revealed that the therapeutic dose of PC-SA used here has no potential toxic effect. Very interestingly, a dose escalation study of PC-SA in mice showed that the mice could tolerate up to 10 times the therapeutic dose without reaching LD50.

The high percentage of PS on the tumor vasculature has been utilized previously for tumor inhibition by targeting it with anti-PS monoclonal antibodies.[13,15] With support of our *in vitro* data, we can postulate that PC-SA also has a similar mode of target selectivity *in vivo*. Unlike the *in vitro* validation, here we could not block PS with its known antibodies because it would, in turn, result in tumor

inhibition. Previous studies illustrate encapsulation of the drug into liposomes or dendrimers only for targeting the drug to the tumor site and to prolong the blood circulation time; in addition, they utilized multiple and high-dose administration.[19,45–47] In contrast, PC-SA liposomes themselves have anticancer efficacy. Thus, a low dose of a single injection of CPT in PC-SA administered in the EAC tumor model and a double dose of PC-SA-entrapped CPT and DOX in the B16F10 mouse melanoma model successfully amplified the therapeutic effects of the drugs with better efficacies than their previous liposomal formulations.[19,32,45,46] It should be noted that the tumor models used in this study, especially the B16F10 melanoma model, are very aggressive tumors, and untreated animals die within 30–35 days of induction of tumor. Thus, the most significant advantage of this study is delayed tumor growth and potential enhancement of the survival of the animals without any substantial sign of toxicity or relapse of the tumor. Our recent studies provide evidence that PC-SA liposomes have significant antitumor immune activity, as also reported by Gerber et.al[13] (data not shown). These findings, together with favorable outcomes of safety, and pharmacology studies in mice encouraged the preclinical translation of this concept. Notably, a graded dose of PC-SA, when tested on primary leukemic cells of AML patients, demonstrates effective killing *in vitro*. Further detailed studies will be required to validate the clinical potentials.

MATERIALS AND METHODS

Preparation and Characterization of Liposomes

Liposomes were prepared with PC (20 mg). PC contains approximately 33% 16:0 (palmitic), 13% 18:0 (stearic), 31% 18:1(oleic), and 15% 18:2 (linoleic) acids; other fatty acids are minor contributors. The chain length of palmitic acid is 16 carbons, that of stearic acid is 18 carbons, that of oleic acid is 18 carbons, and that of linoleic acid is 18 carbons in association with SA (2 mg; SA having an acyl chain length of 18 carbons), Chol (3 mg), or PS (5 mg; PS contains 7% 18:3 alphalinolenic acid and 47% 18:2 linoleic acid, so the chain lengths of linolenic and linoleic acids are 18 carbons) CTAB (2.84 mg), DTAB (2.4 mg), DDAB (4.9 mg), or DOTAP (5.46 mg) at a molar ratio of 7:2. SA was procured from Fluka, and other lipids were procured from Sigma-Aldrich as described previously.[27,48–50] In brief, liposomes were prepared by adding lipids in chloroform and allowed to dissolve completely, followed by evaporating the organic solvent to form a thin film in a round-bottom flask. The film, dried overnight in a vacuum desiccator, was rehydrated in 1 mL of 20 mM PBS (pH 7.4), and the suspension was sonicated for two cycles of 30 s with a 30-s interval on ice using a probe sonicator (Misonix, Microson; output energy, 4 W), followed by incubation for 2 hr at 4°C before use. CPT-encapsulated PC-SA liposomes were prepared by adding DMSO and methanolic solution of 1 mg/mL of CPT to the lipids.[27,46] DOX was entrapped in PC-SA by hydrating the lipid film with 20 mM PBS containing 1 mg/mL of DOX.[27,47] The excess drugs were separated by two successive washings in PBS by ultracentrifugation (100,000 × *g*, 30 min for PC-SA-CPT and 45 min for PC-SA-DOX, 4°C). The concentrations of the stock solutions of all liposomes formed were 20 mg/mL with respect to PC. For the preparation of rhodamine B (red fluorescence) PC-SA liposome, the lipid film containing PC and SA was hydrated with PBS containing 1 mg/mL of rhodamine B. For the preparation of rhodamine123 or fluorescein isothiocyanate (FITC, green fluorescence) PC-SA liposome, an ethanolic solution of 1 mg/mL of rhodamine123 or FITC was added to the lipids in the respective organic solvent, followed by formation of a thin film.[27,51] The unentrapped fluorochromes were separated by two successive washings in PBS by ultracentrifugation (100,000 × *g*, 1 hr, 4°C).

Particle size distribution (for measuring the hydrodynamic diameter) and zeta potential of PC-SA, PC-PS liposomes, and liposomal mixture containing equal amounts of PC-SA (7:2) and PC-PS (7:2) liposomes incubated for 30 min were determined by laser DLS (Malvern Instruments, Zeta sizer, Nano-ZS, model ZEN 3600).

Morphological analyses of PC-SA liposomes were performed by AFM studies as reported previously with slight modifications.[52] In brief, liposomal dispersion (1:100 dilution in Milli-Q water) was placed on mica sheets (freshly cleaved) and dried for the removal of water. Then samples were subjected to AFM analysis (Bruker, USA).

PS Exposure

For annexin V binding, cultured cells with ~90% confluence were removed gently from the plate, dispensed into fresh medium, and washed once. Adherent cultured cells were treated with Accutase (Invitrogen) for 2–3 min at 37°C. 10^6 cells were re-suspended in 1 mL of 1 × binding buffer (BD Biosciences, USA). 100 µL of cell suspension was stained with 5 µL annexin V-FITC and incubated at room temperature (RT) for 5 min in the dark. Analysis of the PS surface content of the cells was performed with a flow cytometer (Becton Dickinson, USA). 10,000 events were collected, and analysis was done with FACS Diva software (Becton Dickinson, USA).[6]

Role of PS in Interaction with Cationic Liposomes

To confirm that PC-SA liposomes directly interact with the surface-exposed PS of cancer cells, 1×10^5 B16F10 cells were seeded on coverslips overnight to adhere. The next day, cells were treated with 15 µg/mL of annexin V and incubated for 30 min at RT to block the surface PS of the cells. Control cells were kept without annexin V. After a PBS wash, cells were incubated with 60 µg/mL of PC-SA or PC-CTAB liposomes conjugated with a red fluorescent dye, rhodamine B,[53] for 2 hr. Cells were fixed with 4% formaldehyde, and their nuclei were stained with DAPI. Cells were visualized under a high-resolution confocal microscope (Leica TCS SP8, software LAS-X) at 540 nm excitation and 625 nm emission wavelength using a 63×/1.40 numerical aperture (NA) oil immersion objective.

The effect of PC-PS liposomes on the anticancer activity of PC-SA liposomes was determined by incubation with 120 µg/mL of PC-SA liposomes for 30 min, with different concentrations of PC-PS liposomes ranging from 15 µg/mL to 240 µg/mL. 5×10^5/mL B16F10, K562, C6 glioma, and U937 cells were added, and viability was assayed after 2 hr by 3-(4,5-dimethyl-2-thiazolyl)-2,5-diphenyl-2H-tetrazolium bromide (MTT) reduction.[54]

To observe the effect of annexin V on PC-SA anticancer activity, B16F10, K562, C6 glioma, and U937 cell suspensions in binding buffer were incubated with or without annexin V at RT for 30 min. Cells were incubated with concentrations of PC-SA liposomes ranging from 20 μg/mL to 140 μg/mL with respect to PC for another 2 hr. Viability of the cells was assayed by MTT reduction.

To observe the effect of anti-PS antibodies on PC-SA anticancer activity, B16F10, K562, C6 glioma, and U937 cell suspensions were incubated with or without anti-PS antibodies clone 1H6 (host, mouse; isotype, immunoglobulin G [IgG]; Upstate) at RT for 30 min. Cells were incubated with concentrations of PC-SA liposomes ranging from 20 μg/mL to 140 μg/mL with respect to PC for another 2 hr. The viability of the cells was assayed by MTT reduction.[54]

Flow Cytometry of B16F10 Cells Incubated with PC-SA Liposomes

To measure the levels of cellular uptake of the liposomes, B16F10 cells were incubated with 60 μg/mL of PC-SA-Rhodamine123 liposomes for 1 hr at 37°C. Unbound liposomes were removed by washing to prevent further binding of liposomes with the cell surface and then kept at 37°C for another 1 hr to allow entry of the surface-bound liposome inside the cell. In the inhibition experiment, cells were incubated with amiloride (500 μM), chlorpromazine (31 μM), or cytochalasin D (500 μM) for 1 hr before addition of liposomes. After incubation, the cells were detached using cell dissociation solution, washed with PBS three times, and subjected to flow cytometry analysis (BD Biosciences).[55]

Mechanistic Studies

To determine the mechanism of killing of PC-SA liposomes, we performed a series of assays designed to assess multiple and sequential events that occur during programmed cell death. Following treatment of cells with a single or graded dose of PC-SA liposomes, the reduction in mitochondrial membrane potential ($\Delta\psi$) in B16F10, K562, and U937 was analyzed using JC-1 dye by flow cytometry (BD MitoScreen Flow Cytometry Mitochondrial Membrane Potential Detection Kit).[56] Release of ROS of PC-SA-treated cells (B16F10, K562, U937, and RAW 264.7 cell lines and normal hPBMCs) was determined by loading cells with H2DCFDA, and fluorescence was measured through a spectrofluorimeter (LS 3B, PerkinElmer, USA) using 499 nm as excitation and 520 nm as emission wavelengths. Data obtained as fluorescence intensity units were normalized and expressed as 100%.[57] Western blot analysis was carried out as described previously[58] to determine the expression of apoptotic markers like p-ERK, p-p38, cleaved caspase-3, cleaved caspase-9, cleaved PARP, and p-AKT in U937, K562, B16F10, and RAW 264.7 cells. To assess the caspase, MAPK, and PI3K pathway-dependent mode of cell death, K562 and B16F10 cells were preincubated with the pancaspase inhibitor Z-VAD-FMK, the p38 inhibitor SB203580, the ERK inhibitor PD98059, or the PI3K inhibitor LY294002 and subsequently incubated with different concentrations of PC-SA liposomes for 2 hr. The viability of the cells was checked by MTT assay. Apoptotic population was determined through annexin V/propidium iodide (PI) staining in treated and untreated B16F10, K562, and U937 cells and normal hPBMCs (BD Pharmingen) and then analyzed on FACS Diva software (Becton Dickinson, USA). Similarly, the percentage of apoptotic cells was determined by flow cytometric analysis of the sub-G0/G1 and G2M DNA population in cell cycle histograms as described in detail elsewhere.[59]

Detection of Morphological Changes in U937 Cells on Treatment with PC-SA Liposomes by Transmission Electron Microscopy

The surface morphology of PC-SA liposome-treated cancer cells was studied by transmission electron microscopy (TEM). Briefly, after treatment with 140 μg/mL of PC-SA for 4 hr, cells were fixed in 3% glutaraldehyde in PBS, post-fixed with 1% OsO_4 for 16–20 hr, gradually dehydrated in ethanol, and finally embedded in SPURRT resin. Thin-cut sections were stained with uranyl acetate and lead acetate and observed in a JEOL-100CX electron microscope.[60]

Cell Proliferation and Viability Assays

Cells were seeded at 5×10^5/mL concentration per well in 96-well plates and treated with PC-SA liposomes (20–350 μg/mL with respect to PC), CPT and DOX (1–7 μg/mL) entrapped in PC-SA liposomes (20–140 μg/mL), free DOX (500–1,000 μg/mL), and free CAMPTOSAR (irinotecan HCl), which is a semisynthetic derivative of CPT (500–10,000 μg/mL). After 2 hr of treatment, the effects on cell viability were determined by MTT assay.[59] EC_{50} values were determined by nonlinear regression analysis of the concentration-response data. The cell viability effect of neutral liposomes on cancerous cells was determined by treating the cells with PC-Chol liposomes (20–140 μg/mL with respect to PC).

Hemocompatibility Study

Different concentrations (20–140 μg/mL) of PC-SA liposomes were separately suspended in 20 mM of PBS. Healthy human blood was obtained, and red blood cells (RBCs) were collected by the density sedimentation on Histopaque-1077 ($400 \times g$, 30 min at RT). The collected RBCs were diluted in PBS to 10% v/v solution. The RBC suspension was incubated with PBS (negative control), 1% Triton X-100 (positive control), and different concentrations of PC-SA. The hemocompatibility of PC-SA liposomes was analyzed according to previous reports.[61,62]

Cell Lines and Cells

Cells of different genetic background (like the murine melanoma B16F10, human neuroblastoma SH5YSY, colorectal adenocarcinoma SW480, human colon carcinoma HCT116, human liver cancer HepG2, human cervical carcinoma HeLa, human breast cancer MCF7, rat C6 glioma, adenogastric carcinoma AGS, HEK, and mouse fibroblast NIH 3T3 cell lines) were maintained in DMEM (Gibco) supplemented with 10% fetal bovine serum (Sigma), sodium pyruvate, 2 mM L-glutamine, penicillin, and streptomycin. The murine macrophage cell line RAW 264.7, the MOLT-3 cell line (derived from human acute lymphoblastic leukemia), the human leukemia cell line K-562, and the human lymphoma cell line U-937 were maintained in RPMI 1640 medium (Sigma) supplemented with 10% fetal

bovine serum, sodium pyruvate, 2 mM L-glutamine, penicillin, and streptomycin. The cells were incubated at 37°C in a humidified atmosphere of 5% CO_2 in air. Rat brain astrocytes were obtained from cerebral cortices of 0-day-old rats as described earlier[63] and maintained in DMEM supplemented with 10% fetal bovine serum (FBS). EAC cells were maintained *in vivo* in Swiss albino mice by intraperitoneal transplantation of 2×10^6 cells per mouse every 15 days. Cells were obtained from the peritoneal fluid after 15 days, washed in 0.02 M PBS, and resuspended in RPMI medium supplemented with 10% FBS. hPBMCs were obtained from healthy donors by density sedimentation on Histopaque-1077 as described previously[64] and resuspended in RPMI medium supplemented with 10% FBS. All of the abovementioned cell lines were procured from the ATCC or National Centre for Cell Science (NCCS) Pune and maintained according to their recommendations.

Antibodies

Antibodies used for quantitative immunoblots were as follows: p-ERK1/2 (Cell Signaling Technology, 9101, 1:1,000), cleaved caspase-3 (Cell Signaling Technology, 9661, 1:1,000), cleaved caspase-9 (Cell Signaling Technology, 9501, 1:1,000), cleaved PARP (Cell Signaling Technology, 9541, 1:1,000), p-p38 (Santa Cruz Biotechnology, sc-17852-R, 1:1,000), p-AKT (Cell Signaling Technology, 13038), and β-actin (Cell Signaling Technology, 4970, 1:1,000). Immunoblots were performed with secondary rabbit or mouse monoclonal antibodies.

In Vivo Acute Toxicity (LD50) Assay with PC-SA Liposomes

To select the dose for *in vivo* evaluation, an acute toxicity test was performed with 220 mg of PC-SA. PC-SA liposomes (220 mg) were administered to four normal healthy Swiss albino mice i.v. within 24 hr. After administration, the animals were observed for 1 day to see whether this dose killed 50% of the animals in the experimental group. This is the LD_{50} of PC-SA. Simultaneously, observation of surviving animals was continued for another 15 days to see whether they were dying. At the same time, we checked whether any salivation, lacrimation, or skin rash occurred. After 15 days, normal and experimental mice were sacrificed, and all vital organs were taken out and checked for toxicity through histopathological analysis. The above toxicity test was performed according to guidance for acute toxicity testing for pharmaceuticals (Centre for Drug Evaluation and Research, August 1996).

In Vivo EAC Trials

We conducted all animal studies in accordance with the guidelines approved by the Indian Animal Ethics Committee (IAEC) and approval from the committee for the purpose of control and supervision of experiments on animals (CPCSEA; New Delhi). Six-week-old Swiss albino mice were inoculated with 2×10^6 EAC cells intraperitoneally in 0.02 M PBS. All experiments were conducted using three to five mice per group. Liposomes were formulated for i.v. dosing in 0.02 M PBS. 22 mg of PC-SA liposomes (which is 10 times less than the dose used in the acute toxicity study), 20 mg/kg of irinotecan HCl (a semisynthetic derivative of CPT), and 20 mg/kg of CPT entrapped in 22 mg of PC-SA liposomes were administered on day 3 i.v. in all studies. The animals were observed for 3 weeks to check for the effect of PC-SA, PC-SA-CPT liposomes, and free irinotecan HCl on the body wt of EAC-bearing mice. Animals were then sacrificed and photographed. The mice were dissected, and the ascitic fluid was collected. The fluid volume was measured in a graduated centrifuge tube, and packed cell volume was determined after centrifuging the cells at 1,000 rpm for 5 min. The cells from the preceding test were stained with trypan blue dye. The cells that took up the dye were non-viable, whereas those that did not were viable. Viable and nonviable cells were counted. Another set of 10 animals in each group was observed for survivability over a period of 75 days.

Plasma Pharmacokinetics and Biodistribution (Pharmacodynamics) Study

For plasma pharmacokinetics, normal Swiss albino mice were injected i.v. with a single dose of 20 mg/kg of CPT entrapped in 22 mg of PC-SA liposomes or 20 mg/kg of irinotecan HCl. At scheduled time points (15 min, 2 hr, 4 hr, 6 hr, and 24 hr), 300 μl of blood was withdrawn from each animal via the tail vein. Blood was processed for plasma. Proteins were precipitated by adding a mixture of methanol and acetonitrile (50:50). The suspension was centrifuged at 9,400 × *g* for 4 min.[65] To determine the level of CPT, the supernatant was analyzed by high-performance/pressure liquid chromatography (HPLC) using a mobile phase consisting of water and acetonitrile (60:40) at a flow rate of 1.0 mL/min and UV detection at 254 nm.[66]

For the biodistribution study, EAC-bearing Swiss albino mice were injected i.v. with 20 mg/kg of CPT entrapped in 22 mg PC-SA and 20 mg/kg body wt of irinotecan HCl. The liver, spleen, lungs, brain, heart, kidneys, and EAC peritoneal fluid were taken out at different time points (2, 4, and 7 hr). Tissue samples were weighed and homogenized by adding 400 μL of tissue lysis buffer and 100 μL of 0.1 N HCl. The homogenate was centrifuged at 14,000 rpm for 30 min at 10°C. Eight hundred microliters of cold methanol was added to 200 μL of supernatant to precipitate tissue proteins. The mixed solution was centrifuged at 14,000 rpm for 15 min at 10°C.[67] EAC peritoneal fluid was taken out by injecting cold methanol intraperitoneally. The fluid was weighed and centrifuged as above. All supernatants were collected to determine the level of CPT and irinotecan by HPLC as mentioned above.

Murine B16F10 *In Vivo* Tumor Model

To establish the therapeutic effects of liposomes on B16F10 melanoma tumor proliferation *in vivo*, C57BL/6 mice were injected s.c. in the left flank with 1×10^6 B16F10 cells on day 0 and then treated s.c. at the tumor site on days 3 and 16, with another set of mice treated similarly on days 7 and 16 when tumors were palpable (i.e., around 65–85 mm^3 in size) with 60 mg/kg of PC-SA liposomes alone, 8.4 mg/kg of free irinotecan HCl, 2.8 mg/kg of free DOX, 8.4 mg/kg of CPT entrapped in 60 mg/kg of PC-SA liposomes, and 2.8 mg/kg of DOX entrapped in 60 mg/kg of PC-SA liposomes. Untreated mice injected with B16F10 cells were kept as a control. Tumor volumes were determined every week until 24 days by measuring (length × width2 × 0.52) in cubic millimeters. TGI was calculated

using the following equation: TGI = (1 − mean tumor volume of the treated group / mean tumor volume of the vehicle control group) × 100. After 24 days of tumor inoculation, treated mice were sacrificed and photographed, and tumor wt were observed. For the lifespan study, the experiment with another set of 10 animals in each group was terminated on day 110.

Confocal Microscopic Analysis of the Uptake of PC-SA-DOX and Free DOX by B16F10 Tumor Cells

To visualize the intratumoral distribution of PC-SA-DOX and free DOX, C57BL6 mice were injected with B16F10 cells s.c. When the tumor volume reached 2000 mm^3 (so that enough cells could be isolated from the tumor mass), mice were injected s.c. at the tumor site with 4 mg/kg of free DOX or DOX entrapped in 11 mg of PC-SA liposome (these amounts of liposomes and drug were used only to visualize their uptake in the TCs at different time points and are not the therapeutic doses). Mice were sacrificed at the 2-, 4-, and 8-h time points, and tumors were dissected. TCs were isolated from the solid tumor mass to obtain a single-cell suspension culture and seeded on coverslips to adhere overnight. The next day, the adhered cells were fixed with 4% paraformaldehyde, stained with DAPI (nucleus stain), and visualized under a confocal microscope (Leica TCS SP8, software LAS-X at 488 nm excitation and 565-630 nm emission wavelengths using a 63×/1.40 NA oil immersion objective) to detect the presence of doxorubicin in B16F10 TCs.

Confocal Microscopic Analysis of the Uptake of PC-SA Liposomes by Tumor Cells and ECs

To detect the uptake of PC-SA liposomes by TCs and ECs, B16F10 tumor-induced (volume, 2,000 mm^3) C57BL6 mice were injected at the tumor site with 11 mg of PC-SA-FITC liposomes (the dose of PC-SA here is not the therapeutic dose but was chosen only to detect its uptake under the microscope). 2 hr after injection, the tumor mass was taken out, and cells were isolated in the form of single-cell suspension. Cells were seeded on coverslips overnight to adhere. The next day, cells were fixed with 4% paraformaldehyde for 20 min, followed by washings with PBS. 1% BSA solution was used for blocking, followed by washing, and cells were then incubated with anti-CD31 rabbit monoclonal antibodies (Cell Signaling Technology), which is an EC marker (1:100 dilution) for 2 hr at RT. After the PBS wash, cells were incubated with Texas red-coupled anti-rabbit IgG secondary antibodies (Santa Cruz, 1:100 dilution) for 1 hr. Cells were washed thoroughly in PBS three times and stained with DAPI, and the coverslips were mounted on glass slides and observed under a confocal microscope (Leica TCS SP8, software LAS-X) at 490 nm excitation and 525 nm emission wavelengths for FITC to detect the uptake of PC-SA and at 596 nm excitation and 615 nm emission wavelength for Texas red to detect the presence of ECs with a 63×/1.40 NA oil immersion objective).

H&E and Immunohistochemistry Staining of Tumor Tissue

Formalin-fixed tissues were obtained on day 24 after sacrificing B16F10 tumor-induced untreated C57BL6 mice or mice treated s.c. with double injection of 60 mg/kg of PC-SA liposomes alone, 2.8 mg/kg of free DOX, and 2.8 mg/kg of DOX entrapped in 60 mg/kg of PC-SA liposomes. Tissues were embedded in paraffin and then sectioned for H&E staining, and images were taken at 40× magnification under a microscope.

For immunohistochemistry (IHC) staining, paraffin-embedded sections of B16F10 tumor tissues of untreated and PC-SA-, DOX- or PC-SA-DOX-treated (with doses as mentioned above) mice as well as normal tissue were deparaffinized and hydrated, followed by antigen retrieval. Endogenous peroxidase was inactivated by hydrogen peroxide for 5–8 min, followed by washing for 5 min. Tumor tissue sections were treated with monoclonal mouse anti-human CD31 (clone JC70A, ready to use, Dako) for 30 min, followed by washing for 5 min. Tumor tissue sections were incubated with horseradish peroxidase-conjugated anti-human secondary antibody (Dako) for 30 min, followed by washing. Visualization of the slides was achieved with diaminobenzidine (DAB), and images were taken at 40× magnification under a microscope.

PC-SA Liposome Radiolabeling Experiments

Radiolabeling of PC-SA liposomes was done by following a previously reported method.[68] Nitrogen purging prior to mixing was carried out to degas all solutions. To 100 μL of ^{99m}Tc (74 MBq) in saline, 5 mg of solid sodium borohydride was added directly with continuous stirring, followed by immediate addition of 500 μL of the liposome solution (25 mg/mL PC-SA with respect to PC was dissolved in Tris-HCl buffer [pH 7.4]). The solution was stirred for 45 min at RT. The contents were filtered using a 0.22-μm filter (Millipore, Carrigtwohill, Ireland), transferred into an evacuated sterile sealed vial, and used for further experiments.

Quality Control and Stability Study

Quality control was performed by following a method described earlier.[69] The labeling efficiency of ^{99m}Tc to PC-SA liposomes was assessed by ascending instant thin-layer chromatography (ITLC) using silica gel (SG) plates. The ITLC-SG was performed using acetone as the mobile phase. Approximately, 2–3 μL of the radiolabeled complex was applied at the bottom point, 1.0 cm from the end of an ITLC strip. The strip was developed until the solvent front reached 8.5 cm from the origin. The labeling efficiency was estimated after dividing the ITLC sheets into two equal halves and counting the radioactivity of each segment using a γ ray spectrometer (GRS 23C, Electronic Corporation of India). The stability of ^{99m}Tc-LP was checked for 6 hr at RT. The labeling efficiency was calculated using the following equation:

$$\text{Labelling Efficiency}(\%) = [(\text{Total counts} - \text{counts of free pertechnetate})/\text{Total counts}] \times 100\%. \quad \text{(Equation 1)}$$

Tumor Imaging by Gamma Scintigraphy

Imaging studies were performed on B16F10 tumor-bearing C57BL/6 mice at Thakurpukur Cancer Research Centre (Regional Radiation Monitoring Centre, Kolkata, India) under a dual-head gamma

camera (GE Hawkeyes, Pittsburgh, USA). $^{99\,m}$Tc-PC-SA liposomes (approximately 100 μCi) were injected s.c. at the site of the tumor (volume, 4,000 mm^3) of the mouse. The animal was placed in a typical position for planar imaging under a small field of view of the experimental gamma camera, suitable for both planar and tomographic imaging. A whole-body image acquisition study was done at 5 min, 1 hr, 2 hr, and 6 hr after injection, and the scan time was 1 min. Image data were obtained and analyzed using a gamma camera (GE Hawkeyes) fitted with a low-energy, high-resolution, all-purpose collimator using the static procedure of the Xeleris Workstation (Functional Imaging) system.

Clinical Samples

Fresh peripheral blood samples were donated by 3 AML and 3 acute promyelocytic leukemia patients with stable phase of the disease, admitted to the Employee State Insurance (ESI) Hospital (Sealdah, Kolkata) before receiving any treatment. Peripheral blood samples were collected with due approval from the human ethics committee of the respective institutes, and all experiments with human blood were conducted under an approved institutional human ethics committee protocol. hPBMCs were isolated by density sedimentation on Histopaque-1077 as described previously,[64] resuspended in RPMI medium supplemented with 10% FBS, and checked for viability by MTT assay.

In Vivo Studies on K562 Xenografts

K562 cells were suspended to 1×10^7 cells/mL in Matrigel (1 volume of cells with 1 volume of cold Matrigel). Nude female mice 6 to 7 weeks of age (National Institute of Nutrition, Hyderabad, and National Institute of Immunology, New Delhi, India) were given injections of 0.1 mL of this suspension. On days 7 and 16, mice were administered s.c. 60 mg/kg of PC-SA liposomes alone, 2.8 mg/kg of free DOX, and 2.8 mg/kg of DOX entrapped in 60 mg/kg of PC-SA liposomes. Untreated mice served as a control. On day 24, mice were sacrificed and photographed, and tumor volume was measured.

Toxicity Tests across *In Vivo* Models

For toxicity tests, normal healthy Swiss albino mice were injected i.v. with a single dose of free irinotecan HCl (20 mg/kg), PC-SA only (22 mg/mouse), or PC-SA (22 mg/mouse)-associated CPT (20 mg/kg), and C57BL/6 mice were s.c. injected twice with the liposomal formulations as used for therapy. After 2 weeks, 300 μL of the blood was collected through the tail vein. Urea, creatinine, aspartate amino transferase (AST, also called SGOT), alanine aminotransferase (ALT, also called SGPT), and alkaline phosphatase from serum were analyzed on day 15 after treatment using diagnostic kits (Randox Laboratories, Northern Ireland). Toxicity studies were carried out on normal healthy mice and not on tumor-bearing mice because these toxicity parameters are already elevated in tumorigenic mice, and, thus, it is difficult to compare the toxicity of the formulations.[70]

Histological Analysis of Organ Toxicity

Liver, lung, brain, kidney, spleen, and heart samples collected after 15 days from mice injected with PC-SA (22 mg or 222 mg), 20 mg/kg of irinotecan HCl, and 20 mg/kg of CPT entrapped in 22 mg PC-SA were fixed in 10% buffered formalin, processed through conventional histological techniques, and stained with H&E. Microscopy was performed using an optical microscope equipped with a camera.

Statistical Analysis

Testing was performed using GraphPad Prism 5 software (https://www.graphpad.com) software. Statistical significance (***$p < 0.0001$, all other p values as stated) was calculated using Student's t test in the case of two comparison groups and ANOVA with Tukey's correction in the case of more than two comparison groups. SDs are given. Log rank testing was used to analyze survival data.

SUPPLEMENTAL INFORMATION

Supplemental Information includes twelve figures and one table and can be found with this article online at https://doi.org/10.1016/j.omtn.2017.10.019.

AUTHOR CONTRIBUTIONS

Conception and Design, N.A., M.D., and T.S.; Development and Methodology, N.A., M.D., and T.S.; Acquisition of Data, M.D., S.G., M.S., and I.B.; Analysis and Interpretation of Data: M.D., S.G., M.S., and I.B.; Writing, Review, and/or Revision of the Manuscript, S.G., M.D., and N.A.; Administrative, Technical, and Material Support, N.A. and S.B.; Study Supervision, N.A.

ACKNOWLEDGMENTS

The authors are thankful to the Indian Council for Medical Research, the Department of Biotechnology, the Council for Scientific and Industrial Research, and the Department of Atomic Energy (Government of India) for providing fellowship support. The authors acknowledge R. Sinha for critical reading of this manuscript; S.T. Choudhury, R. Sinha, M. Asad, M. Maji, and S. Das for useful discussions; A. Gangopadhyay and S. Mullick for flow cytometry; S. Bhattacharya for confocal microscopy; and A. Laskar for Transmission Electron Microscopy. We would also like to thank J. Midya for assisting with animal studies.

REFERENCES

1. Kenis, H., and Reutelingsperger, C. (2009). Targeting phosphatidylserine in anti-cancer therapy. Curr. Pharm. Des. *15*, 2719–2723.
2. Zwaal, R.F., and Schroit, A.J. (1997). Pathophysiologic implications of membrane phospholipid asymmetry in blood cells. Blood *89*, 1121–1132.
3. Beck, A.W., Luster, T.A., Miller, A.F., Holloway, S.E., Conner, C.R., Barnett, C.C., Thorpe, P.E., Fleming, J.B., and Brekken, R.A. (2006). Combination of a monoclonal anti-phosphatidylserine antibody with gemcitabine strongly inhibits the growth and metastasis of orthotopic pancreatic tumors in mice. Int. J. Cancer *118*, 2639–2643.
4. Utsugi, T., Schroit, A.J., Connor, J., Bucana, C.D., and Fidler, I.J. (1991). Elevated expression of phosphatidylserine in the outer membrane leaflet of human tumor cells and recognition by activated human blood monocytes. Cancer Res. *51*, 3062–3066.
5. Soares, M.M., King, S.W., and Thorpe, P.E. (2008). Targeting inside-out phosphatidylserine as a therapeutic strategy for viral diseases. Nat. Med. *14*, 1357–1362.
6. Riedl, S., Rinner, B., Asslaber, M., Schaider, H., Walzer, S., Novak, A., Lohner, K., and Zweytick, D. (2011). In search of a novel target - phosphatidylserine exposed by non-apoptotic tumor cells and metastases of malignancies with poor treatment efficacy. Biochim. Biophys. Acta *1808*, 2638–2645.

7. Ran, S., Downes, A., and Thorpe, P.E. (2002). Increased exposure of anionic phospholipids on the surface of tumor blood vessels. Cancer Res. *62*, 6132–6140.

8. Schlegel, R.A., and Williamson, P. (2001). Phosphatidylserine, a death knell. Cell Death Differ. *8*, 551–563.

9. Schröder-Borm, H., Bakalova, R., and Andrä, J. (2005). The NK-lysin derived peptide NK-2 preferentially kills cancer cells with increased surface levels of negatively charged phosphatidylserine. FEBS Lett. *579*, 6128–6134.

10. Fernandes, R.S., Kirszberg, C., Rumjanek, V.M., and Monteiro, R.Q. (2006). On the molecular mechanisms for the highly procoagulant pattern of C6 glioma cells. J. Thromb. Haemost. *4*, 1546–1552.

11. Kirszberg, C., Lima, L.G., Da Silva de Oliveira, A., Pickering, W., Gray, E., Barrowcliffe, T.W., Rumjanek, V.M., and Monteiro, R.Q. (2009). Simultaneous tissue factor expression and phosphatidylserine exposure account for the highly procoagulant pattern of melanoma cell lines. Melanoma Res. *19*, 301–308.

12. Dong, H.P., Holth, A., Kleinberg, L., Ruud, M.G., Elstrand, M.B., Tropé, C.G., Davidson, B., and Risberg, B. (2009). Evaluation of cell surface expression of phosphatidylserine in ovarian carcinoma effusions using the annexin-V/7-AAD assay: clinical relevance and comparison with other apoptosis parameters. Am. J. Clin. Pathol. *132*, 756–762.

13. Gerber, D.E., Stopeck, A.T., Wong, L., Rosen, L.S., Thorpe, P.E., Shan, J.S., and Ibrahim, N.K. (2011). Phase I safety and pharmacokinetic study of bavituximab, a chimeric phosphatidylserine-targeting monoclonal antibody, in patients with advanced solid tumors. Clin. Cancer Res. *17*, 6888–6896.

14. Blanco, V.M., Chu, Z., Vallabhapurapu, S.D., Sulaiman, M.K., Kendler, A., Rixe, O., Warnick, R.E., Franco, R.S., and Qi, X. (2014). Phosphatidylserine-selective targeting and anticancer effects of SapC-DOPS nanovesicles on brain tumors. Oncotarget *5*, 7105–7118.

15. He, J., Yin, Y., Luster, T.A., Watkins, L., and Thorpe, P.E. (2009). Antiphosphatidylserine antibody combined with irradiation damages tumor blood vessels and induces tumor immunity in a rat model of glioblastoma. Clin. Cancer Res. *15*, 6871–6880.

16. Zhang, L., Zhou, H., Belzile, O., Thorpe, P., and Zhao, D. (2014). Phosphatidylserine-targeted bimodal liposomal nanoparticles for in vivo imaging of breast cancer in mice. J. Control. Release *183*, 114–123.

17. Qi, X., Chu, Z., Mahller, Y.Y., Stringer, K.F., Witte, D.P., and Cripe, T.P. (2009). Cancer-selective targeting and cytotoxicity by liposomal-coupled lysosomal saposin C protein. Clin. Cancer Res. *15*, 5840–5851.

18. Ayesa, U., Gray, B.D., Pak, K.Y., and Chong, P.L. (2017). Liposomes Containing Lipid-Soluble Zn(II)-Bis-dipicolylamine Derivatives Show Potential To Be Targeted to Phosphatidylserine on the Surface of Cancer Cells. Mol. Pharm. *14*, 147–156.

19. Peer, D., and Margalit, R. (2004). Tumor-targeted hyaluronan nanoliposomes increase the antitumor activity of liposomal Doxorubicin in syngeneic and human xenograft mouse tumor models. Neoplasia *6*, 343–353.

20. Fanciullino, R., and Ciccolini, J. (2009). Liposome-encapsulated anticancer drugs: still waiting for the magic bullet? Curr. Med. Chem. *16*, 4361–4371.

21. Tardi, P., Choice, E., Masin, D., Redelmeier, T., Bally, M., and Madden, T.D. (2000). Liposomal encapsulation of topotecan enhances anticancer efficacy in murine and human xenograft models. Cancer Res. *60*, 3389–3393.

22. Abu Lila, A.S., Ishida, T., and Kiwada, H. (2010). Targeting anticancer drugs to tumor vasculature using cationic liposomes. Pharm. Res. *27*, 1171–1183.

23. Ansell, S.M., Harasym, T.O., Tardi, P.G., Buchkowsky, S.S., Bally, M.B., and Cullis, P.R. (2000). Antibody conjugation methods for active targeting of liposomes. Methods Mol. Med. *25*, 51–68.

24. Chen, Y.Q., Min, C., Sang, M., Han, Y.Y., Ma, X., Xue, X.Q., and Zhang, S.Q. (2010). A cationic amphiphilic peptide ABP-CM4 exhibits selective cytotoxicity against leukemia cells. Peptides *31*, 1504–1510.

25. Dass, C.R., and Choong, P.F. (2006). Targeting of small molecule anticancer drugs to the tumour and its vasculature using cationic liposomes: lessons from gene therapy. Cancer Cell Int. *6*, 17.

26. Thurston, G., McLean, J.W., Rizen, M., Baluk, P., Haskell, A., Murphy, T.J., Hanahan, D., and McDonald, D.M. (1998). Cationic liposomes target angiogenic endothelial cells in tumors and chronic inflammation in mice. J. Clin. Invest. *101*, 1401–1413.

27. Banerjee, A., Roychoudhury, J., and Ali, N. (2008). Stearylamine-bearing cationic liposomes kill Leishmania parasites through surface exposed negatively charged phosphatidylserine. J. Antimicrob. Chemother. *61*, 103–110.

28. Srivastava, S., Somasagara, R.R., Hegde, M., Nishana, M., Tadi, S.K., Srivastava, M., Choudhary, B., and Raghavan, S.C. (2016). Quercetin, a Natural Flavonoid Interacts with DNA, Arrests Cell Cycle and Causes Tumor Regression by Activating Mitochondrial Pathway of Apoptosis. Sci. Rep. *6*, 24049.

29. Pusztaszeri, M.P., Seelentag, W., and Bosman, F.T. (2006). Immunohistochemical expression of endothelial markers CD31, CD34, von Willebrand factor, and Fli-1 in normal human tissues. J. Histochem. Cytochem. *54*, 385–395.

30. Lecaros, R.L., Huang, L., Lee, T.C., and Hsu, Y.C. (2016). Nanoparticle Delivered VEGF-A siRNA Enhances Photodynamic Therapy for Head and Neck Cancer Treatment. Mol. Ther. *24*, 106–116.

31. Huang, X., Bennett, M., and Thorpe, P.E. (2005). A monoclonal antibody that binds anionic phospholipids on tumor blood vessels enhances the antitumor effect of docetaxel on human breast tumors in mice. Cancer Res. *65*, 4408–4416.

32. Liu, X.P., Zhou, S.T., Li, X.Y., Chen, X.C., Zhao, X., Qian, Z.Y., Zhou, L.N., Li, Z.Y., Wang, Y.M., Zhong, Q., et al. (2010). Anti-tumor activity of N-trimethyl chitosan-encapsulated camptothecin in a mouse melanoma model. J. Exp. Clin. Cancer Res. *29*, 76.

33. Zhao, D., Stafford, J.H., Zhou, H., and Thorpe, P.E. (2011). Near-infrared Optical Imaging of Exposed Phosphatidylserine in a Mouse Glioma Model. Transl. Oncol. *4*, 355–364.

34. Judy, B.F., Aliperti, L.A., Predina, J.D., Levine, D., Kapoor, V., Thorpe, P.E., Albelda, S.M., and Singhal, S. (2012). Vascular endothelial-targeted therapy combined with cytotoxic chemotherapy induces inflammatory intratumoral infiltrates and inhibits tumor relapses after surgery. Neoplasia *14*, 352–359.

35. Strieth, S., Eichhorn, M.E., Werner, A., Sauer, B., Teifel, M., Michaelis, U., Berghaus, A., and Dellian, M. (2008). Paclitaxel encapsulated in cationic liposomes increases tumor microvessel leakiness and improves therapeutic efficacy in combination with Cisplatin. Clin. Cancer Res. *14*, 4603–4611.

36. Lin, C.H., Al-Suwayeh, S.A., Hung, C.F., Chen, C.C., and Fang, J.Y. (2013). Camptothecin-Loaded Liposomes with α-Melanocyte-Stimulating Hormone Enhance Cytotoxicity Toward and Cellular Uptake by Melanomas: An Application of Nanomedicine on Natural Product. J. Tradit. Complement. Med. *3*, 102–109.

37. Xing, H., Tang, L., Yang, X., Hwang, K., Wang, W., Yin, Q., Wong, N.Y., Dobrucki, L.W., Yasui, N., Katzenellenbogen, J.A., et al. (2013). Selective Delivery of an Anticancer Drug with Aptamer-Functionalized Liposomes to Breast Cancer Cells in Vitro and in Vivo. J. Mater. Chem. B Mater. Biol. Med. *1*, 5288–5297.

38. Xiong, X.B., Huang, Y., Lu, W.L., Zhang, X., Zhang, H., Nagai, T., and Zhang, Q. (2005). Intracellular delivery of doxorubicin with RGD-modified sterically stabilized liposomes for an improved antitumor efficacy: in vitro and in vivo. J. Pharm. Sci. *94*, 1782–1793.

39. Yuan, F., Leunig, M., Huang, S.K., Berk, D.A., Papahadjopoulos, D., and Jain, R.K. (1994). Microvascular permeability and interstitial penetration of sterically stabilized (stealth) liposomes in a human tumor xenograft. Cancer Res. *54*, 3352–3356.

40. Jithan, A., Madhavi, K., Madhavi, M., and Prabhakar, K. (2011). Preparation and characterization of albumin nanoparticles encapsulating curcumin intended for the treatment of breast cancer. Int. J. Pharm. Investig. *1*, 119–125.

41. Moghimi, S.M., and Patel, H.M. (2002). Modulation of murine liver macrophage clearance of liposomes by diethylstilbestrol. The effect of vesicle surface charge and a role for the complement receptor Mac-1 (CD11b/CD18) of newly recruited macrophages in liposome recognition. J. Control. Release *78*, 55–65.

42. Sonoke, S., Ueda, T., Fujiwara, K., Sato, Y., Takagaki, K., Hirabayashi, K., Ohgi, T., and Yano, J. (2008). Tumor regression in mice by delivery of Bcl-2 small interfering RNA with pegylated cationic liposomes. Cancer Res. *68*, 8843–8851.

43. Harivardhan Reddy, L., Sharma, R.K., Chuttani, K., Mishra, A.K., and Murthy, R.S. (2005). Influence of administration route on tumor uptake and biodistribution of etoposide loaded solid lipid nanoparticles in Dalton's lymphoma tumor bearing mice. J. Control. Release *105*, 185–198.

44. Yoshihara, E., and Nakae, T. (1986). Cytolytic activity of liposomes containing stearylamine. Biochim. Biophys. Acta *854*, 93–101.

45. Niu, M., Naguib, Y.W., Aldayel, A.M., Shi, Y.C., Hursting, S.D., Hersh, M.A., and Cui, Z. (2014). Biodistribution and in vivo activities of tumor-associated macrophage-targeting nanoparticles incorporated with doxorubicin. Mol. Pharm. *11*, 4425–4436.

46. Benkovic, V., Horvat Knezevic, A., Brozovic, G., Knezevic, F., Dikic, D., Bevanda, M., Basic, I., and Orsolic, N. (2007). Enhanced antitumor activity of irinotecan combined with propolis and its polyphenolic compounds on Ehrlich ascites tumor in mice. Biomed. Pharmacother. *61*, 292–297.

47. Al-Jamal, K.T., Al-Jamal, W.T., Wang, J.T., Rubio, N., Buddle, J., Gathercole, D., Zloh, M., and Kostarelos, K. (2013). Cationic poly-L-lysine dendrimer complexes doxorubicin and delays tumor growth in vitro and in vivo. ACS Nano *7*, 1905–1917.

48. Joo, K.I., Xiao, L., Liu, S., Liu, Y., Lee, C.L., Conti, P.S., Wong, M.K., Li, Z., and Wang, P. (2013). Crosslinked multilamellar liposomes for controlled delivery of anticancer drugs. Biomaterials *34*, 3098–3109.

49. Liu, Y., Fang, J., Kim, Y.J., Wong, M.K., and Wang, P. (2014). Codelivery of doxorubicin and paclitaxel by cross-linked multilamellar liposome enables synergistic antitumor activity. Mol. Pharm. *11*, 1651–1661.

50. Moon, J.J., Suh, H., Bershteyn, A., Stephan, M.T., Liu, H., Huang, B., Sohail, M., Luo, S., Um, S.H., Khant, H., et al. (2011). Interbilayer-crosslinked multilamellar vesicles as synthetic vaccines for potent humoral and cellular immune responses. Nat. Mater. *10*, 243–251.

51. Rudra, A., Deepa, R.M., Ghosh, M.K., Ghosh, S., and Mukherjee, B. (2010). Doxorubicin-loaded phosphatidylethanolamine-conjugated nanoliposomes: in vitro characterization and their accumulation in liver, kidneys, and lungs in rats. Int. J. Nanomedicine *5*, 811–823.

52. Bharti, R., Dey, G., Banerjee, I., Dey, K.K., Parida, S., Kumar, B.N., Das, C.K., Pal, I., Mukherjee, M., Misra, M., et al. (2017). Somatostatin receptor targeted liposomes with Diacerein inhibit IL-6 for breast cancer therapy. Cancer Lett. *388*, 292–302.

53. Kang, D.I., Kang, H.K., Gwak, H.S., Han, H.K., and Lim, S.J. (2009). Liposome composition is important for retention of liposomal rhodamine in P-glycoprotein-overexpressing cancer cells. Drug Deliv. *16*, 261–267.

54. Morgan, M.T., Nakanishi, Y., Kroll, D.J., Griset, A.P., Carnahan, M.A., Wathier, M., Oberlies, N.H., Manikumar, G., Wani, M.C., and Grinstaff, M.W. (2006). Dendrimer-encapsulated camptothecins: increased solubility, cellular uptake, and cellular retention affords enhanced anticancer activity in vitro. Cancer Res. *66*, 11913–11921.

55. Nakamura, T., Moriguchi, R., Kogure, K., Shastri, N., and Harashima, H. (2008). Efficient MHC class I presentation by controlled intracellular trafficking of antigens in octaarginine-modified liposomes. Mol. Ther. *16*, 1507–1514.

56. Sawa, A., Wiegand, G.W., Cooper, J., Margolis, R.L., Sharp, A.H., Lawler, J.F., Jr., Greenamyre, J.T., Snyder, S.H., and Ross, C.A. (1999). Increased apoptosis of Huntington disease lymphoblasts associated with repeat length-dependent mitochondrial depolarization. Nat. Med. *5*, 1194–1198.

57. Schenk, B., and Fulda, S. (2015). Reactive oxygen species regulate Smac mimetic/TNFα-induced necroptotic signaling and cell death. Oncogene *34*, 5796–5806.

58. Chang, L., Graham, P.H., Hao, J., Ni, J., Bucci, J., Cozzi, P.J., Kearsley, J.H., and Li, Y. (2013). Acquisition of epithelial-mesenchymal transition and cancer stem cell phenotypes is associated with activation of the PI3K/Akt/mTOR pathway in prostate cancer radioresistance. Cell Death Dis. *4*, e875.

59. Zhou, Y., Han, C., Li, D., Yu, Z., Li, F., Li, F., An, Q., Bai, H., Zhang, X., Duan, Z., and Kan, Q. (2015). Cyclin-dependent kinase 11(p110) (CDK11(p110)) is crucial for human breast cancer cell proliferation and growth. Sci. Rep. *5*, 10433.

60. Tu, S.P., Zhong, J., Tan, J.H., Jiang, X.H., Qiao, M.M., Wu, Y.X., and Jiang, S.H. (2000). Induction of apoptosis by arsenic trioxide and hydroxy camptothecin in gastric cancer cells in vitro. World J. Gastroenterol. *6*, 532–539.

61. Banerjee, I., De, K., Mukherjee, D., Dey, G., Chattopadhyay, S., Mukherjee, M., Mandal, M., Bandyopadhyay, A.K., Gupta, A., Ganguly, S., and Misra, M. (2016). Paclitaxel-loaded solid lipid nanoparticles modified with Tyr-3-octreotide for enhanced anti-angiogenic and anti-glioma therapy. Acta Biomater. *38*, 69–81.

62. Venkatesan, P., Puvvada, N., Dash, R., Prashanth Kumar, B.N., Sarkar, D., Azab, B., Pathak, A., Kundu, S.C., Fisher, P.B., and Mandal, M. (2011). The potential of celecoxib-loaded hydroxyapatite-chitosan nanocomposite for the treatment of colon cancer. Biomaterials *32*, 3794–3806.

63. Hung, S.Y., Liou, H.C., Kang, K.H., Wu, R.M., Wen, C.C., and Fu, W.M. (2008). Overexpression of heme oxygenase-1 protects dopaminergic neurons against 1-methyl-4-phenylpyridinium-induced neurotoxicity. Mol. Pharmacol. *74*, 1564–1575.

64. Saha, S., Mondal, S., Ravindran, R., Bhowmick, S., Modak, D., Mallick, S., Rahman, M., Kar, S., Goswami, R., Guha, S.K., et al. (2007). IL-10- and TGF-beta-mediated susceptibility in kala-azar and post-kala-azar dermal leishmaniasis: the significance of amphotericin B in the control of Leishmania donovani infection in India. J. Immunol. *179*, 5592–5603.

65. Poujol, S., Pinguet, F., Malosse, F., Astre, C., Ychou, M., Culine, S., and Bressolle, F. (2003). Sensitive HPLC-fluorescence method for irinotecan and four major metabolites in human plasma and saliva: application to pharmacokinetic studies. Clin. Chem. *49*, 1900–1908.

66. Barilero, I., Gandia, D., Armand, J.P., Mathieu-Boué, A., Ré, M., Gouyette, A., and Chabot, G.G. (1992). Simultaneous determination of the camptothecin analogue CPT-11 and its active metabolite SN-38 by high-performance liquid chromatography: application to plasma pharmacokinetic studies in cancer patients. J. Chromatogr. A *575*, 275–280.

67. Schluep, T., Cheng, J., Khin, K.T., and Davis, M.E. (2006). Pharmacokinetics and biodistribution of the camptothecin-polymer conjugate IT-101 in rats and tumor-bearing mice. Cancer Chemother. Pharmacol. *57*, 654–662.

68. Banerjee, I., De, K., Chattopadhyay, S., Bandyopadhyay, A.K., and Misra, M. (2014). An easy and effective method for radiolabelling of solid lipid nanoparticles. J. Radioanal. Nucl. Chem. *302*, 837–843.

69. Theobald, A.E. (1990). Textbook of radiopharmacy: theory and practice (New York: Gorden and Breach).

70. Samudrala, P.K., Augustine, B.B., Kasala, E.R., Bodduluru, L.N., Barua, C., and Lahkar, M. (2015). Evaluation of antitumor activity and antioxidant status of Alternanthera brasiliana against Ehrlich ascites carcinoma in Swiss albino mice. Pharmacognosy Res. *7*, 66–73.

OMTN, Volume *10*

Supplemental Information

A Novel Therapeutic Strategy for Cancer Using Phosphatidylserine Targeting Stearylamine-Bearing Cationic Liposomes

Manjarika De, Sneha Ghosh, Triparna Sen, Md. Shadab, Indranil Banerjee, Santanu Basu, and Nahid Ali

SUPPLEMENTARY MATERIALS

Figure S 1: Chemical structure of PC and SA, AFM analysis of PC-SA liposome.

Figure S2: No killing effect of neutral liposome, PC-Chol, on cancer cell lines.

Figure S 3: Size distribution and zeta potential of PC-SA liposomes following incubation with PC-PS liposomes for 30 mins.

Figure S4: Effect of different cationic liposomes on B16F10 cells.

Figure S5: PC-SA killing activity is Caspase, MAPK and PI3K dependent.

Figure S 6: Transmission electron microscopy of U937 cells treated with PC-SA liposomes for 4 h.

Figure S7: Acute toxicity study.

Figure S 8: No increase in body weight between day 0 and 21 of EAC innoculated Swiss albino mice treated with PC-SA-CPT.

Figure S 9: Toxicity study of brain, lungs and heart in normal Swiss albino mice.

Figure S10: Uptake of PC-SA-DOX and free DOX by B16F10 tumor cells:

Figure S 11: Immunohistochemical analysis of tumor and normal tissue sections for expression of CD31 (marker used in vascular tumor).

Figure S 12: Uptake of PC-SA liposome by endothelial cells and tumor cells:

Table S 1: Stability of ^{99m}Tc-PC-SA lipsome at room temperature at different time points.

SUPPLEMENTARY FIGURES

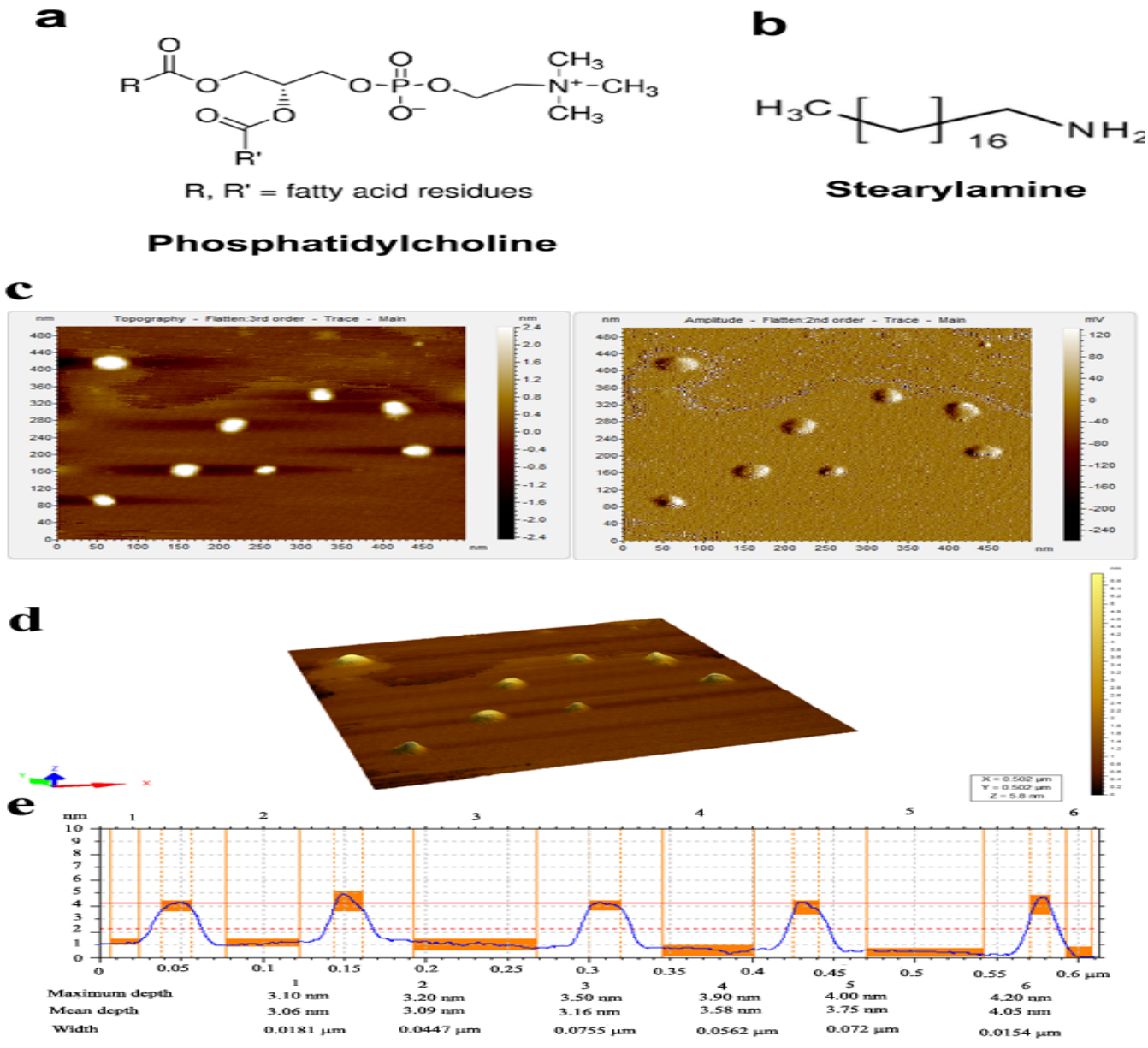

Figure S 1: Chemical structure of PC and SA, AFM analysis of PC-SA liposome (a) Chemical structure of phosphatidylcholine (b) and stearylamine. (c) AFM images presented as two-dimensional graphics showing the clean spherical shaped PC-SA liposome. Topography flattened and amplitude-flattened views of liposomes are shown. (d) 3D image of PC-SA liposome by AFM studies. (e) Horizontal cross sections indicating the height of the liposome from the substratum, i.e., the mica sheet.

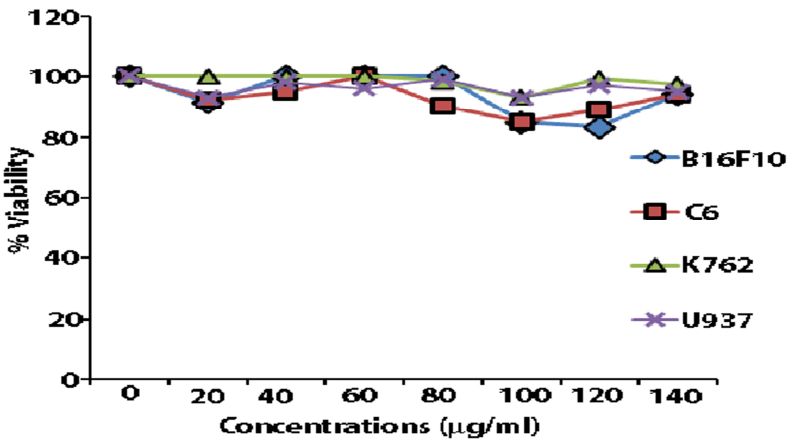

Figure S 2: No killing effect of neutral liposome, PC-Chol, on cancer cell lines. Cell viability of B16F10, rat C6 glioma, K562 and U937 cells following incubation with increasing concentrations (20-140 µg/ml) of PC-Chol liposomes with respect to PC for 2 h. All data represent the mean of three separate experiments with error bars indicating the standard error of the mean.

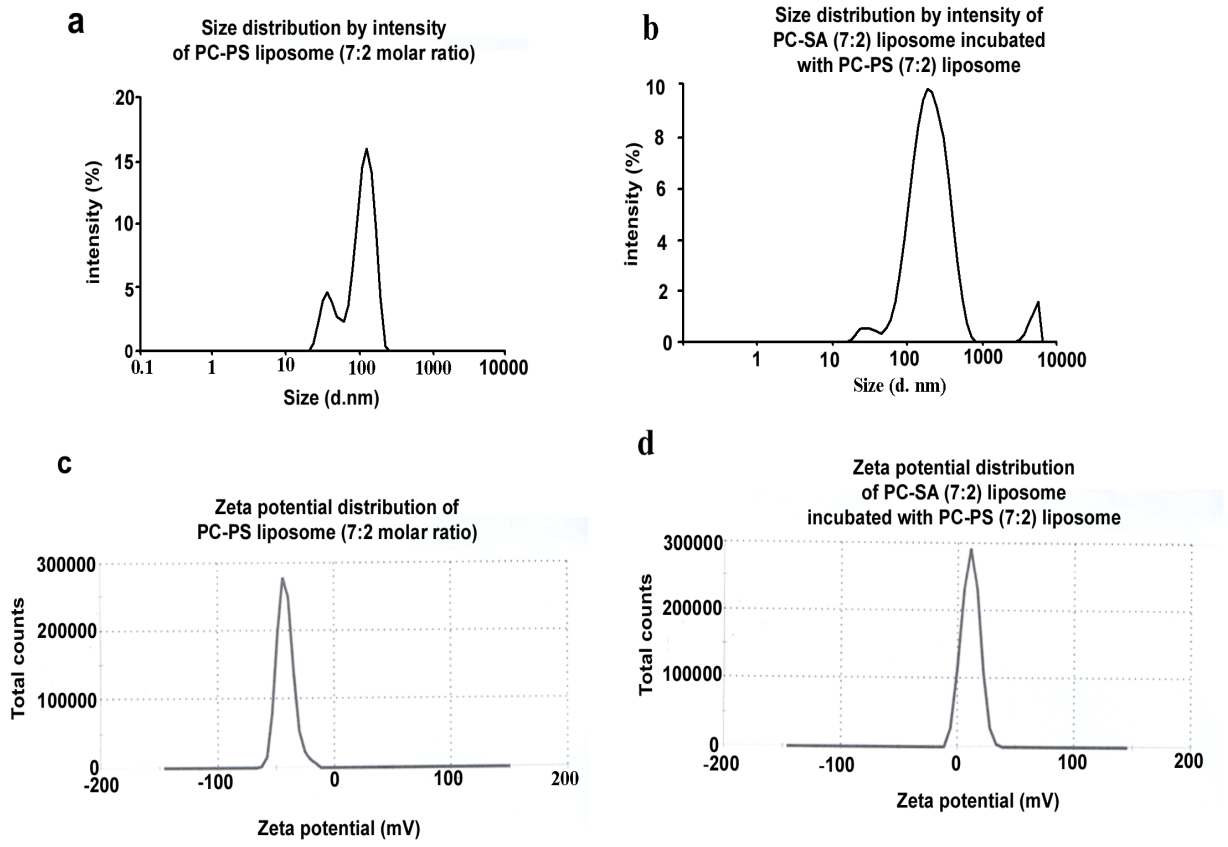

Figure S 3: Size distribution and zeta potential of PC-SA liposomes following incubation with PC-PS liposomes for 30 mins. (a) Size distribution of negatively charge PC-PS liposomes (7:2 molar ratio). (b) Size distribution of PC-SA liposome (7:2 molar ratio) incubated with PC-PS liposome (7:2 molar ratio). (c) Zeta potential of PC-PS liposome. (d) Zeta potential of PC-SA liposome incubated with PC-PS liposome.

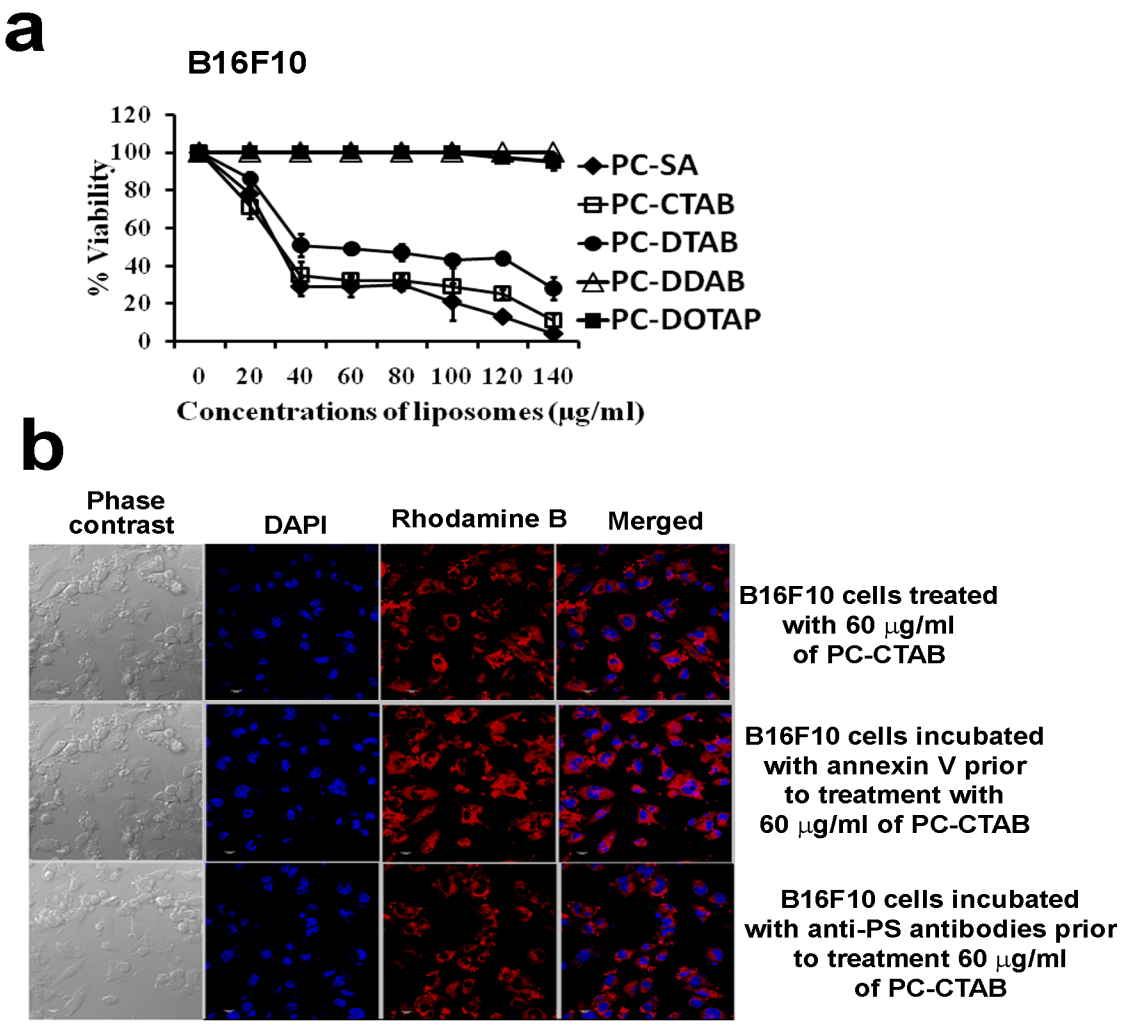

Figure S 4: Effect of different cationic liposomes on B16F10 cells. (a) Viability of B16F10 cells after treatment with graded concentrations of 7:2 molar ratio of PC-SA, PC-CTAB, PC-DTAB, PC-DDAB and PC-DOTAP liposomes with respect to PC for 2 h. Data represent the mean of three separate experiments with error bars indicating the standard error of the mean. (b) Interaction of Rhodamine B PC-CTAB liposomes for 2 h with cancer cell line B16F10 in presence or absence of annexin V or anti-PS antibodies. Cells were visualized under confocal microscope (Leica TCS SP8, software LAS-X), Scale bar: 10 µm.

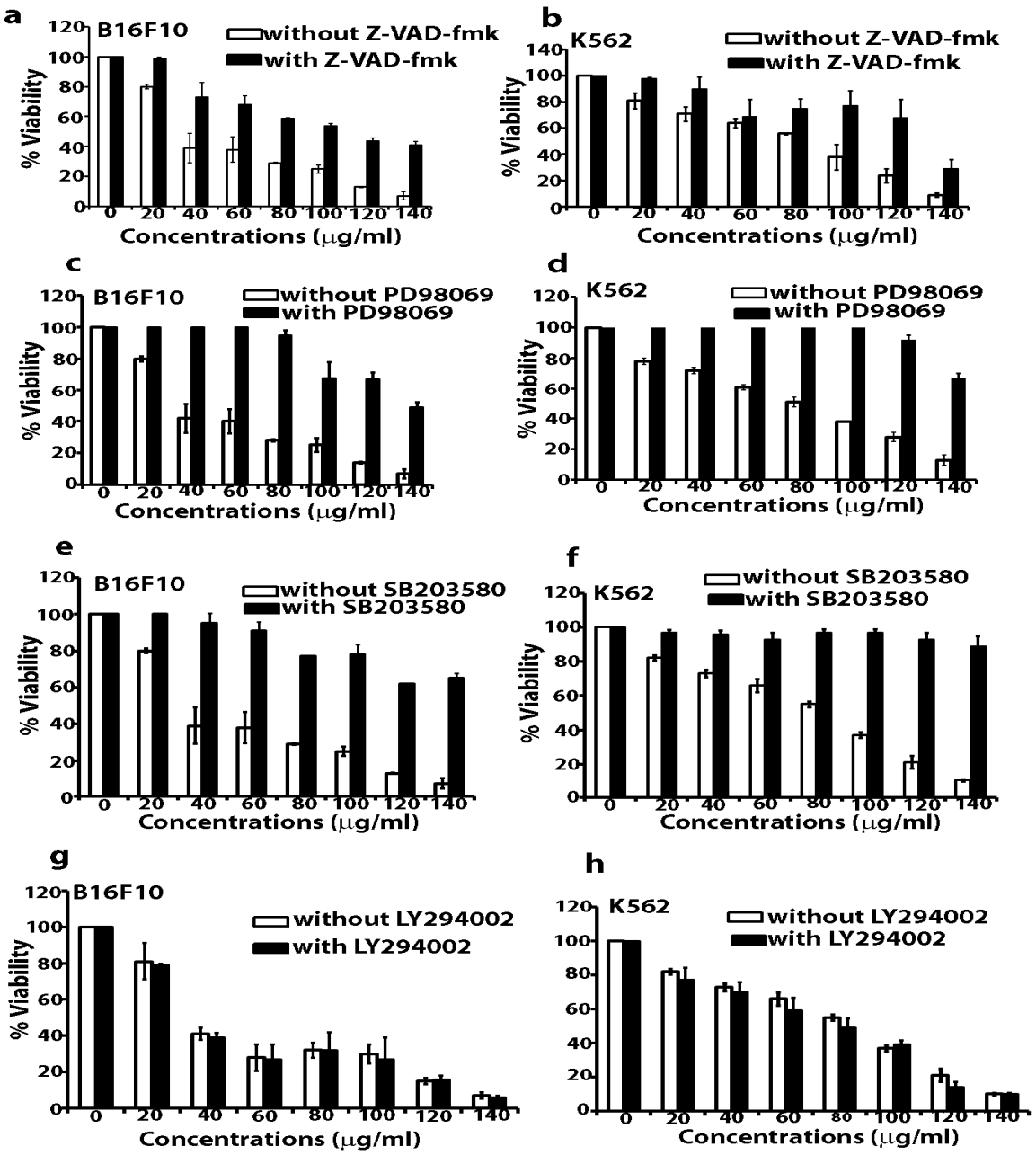

Figure S 5: PC-SA killing activity is Caspase, MAPK and PI3K dependent. (a,c, e, and g) B16F10 and (b, d, f and h) K562 cells were treated with graded doses of PC-SA liposomes (20-140 μg/ml) with respect to PC in the presence or absence of 10 μM of pancaspace inhibitor Z-VAD-fmk, ERK inhibitor PD98069, p38 inhibitor SB203680 and AKT inhibitor LY294002. All data represent the mean of triplicate experiments, with error bars indicating the s.e.m.

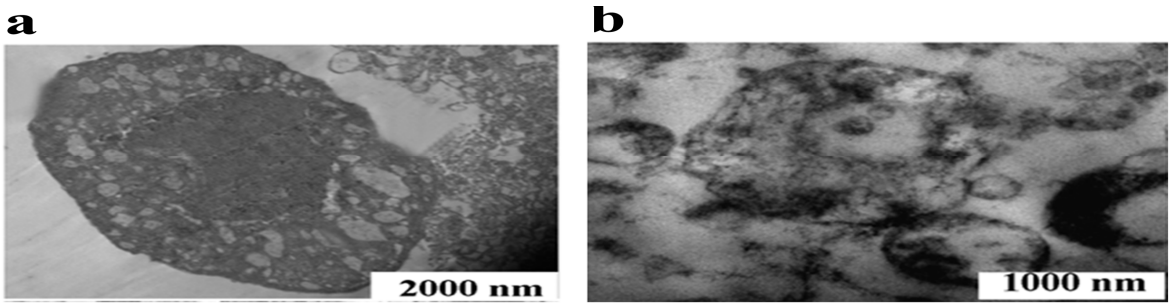

Figure S 6: Transmission electron microscopy of U937 cells treated with PC-SA liposomes for 4 h. U937 cells were incubated for 4 h under standard conditions with medium alone (a), and 140 µg/ml (b) of PC-SA liposomes with respect to PC. Representative of electron micrograph of 140 µg/ml treated cells revealed extensive vacuolization and membrane breakage as well as depletion of electron-dense cytoplasmic material indicating that cell death is in process. Scale bars: 2000 nm (a), 1000 nm (b).

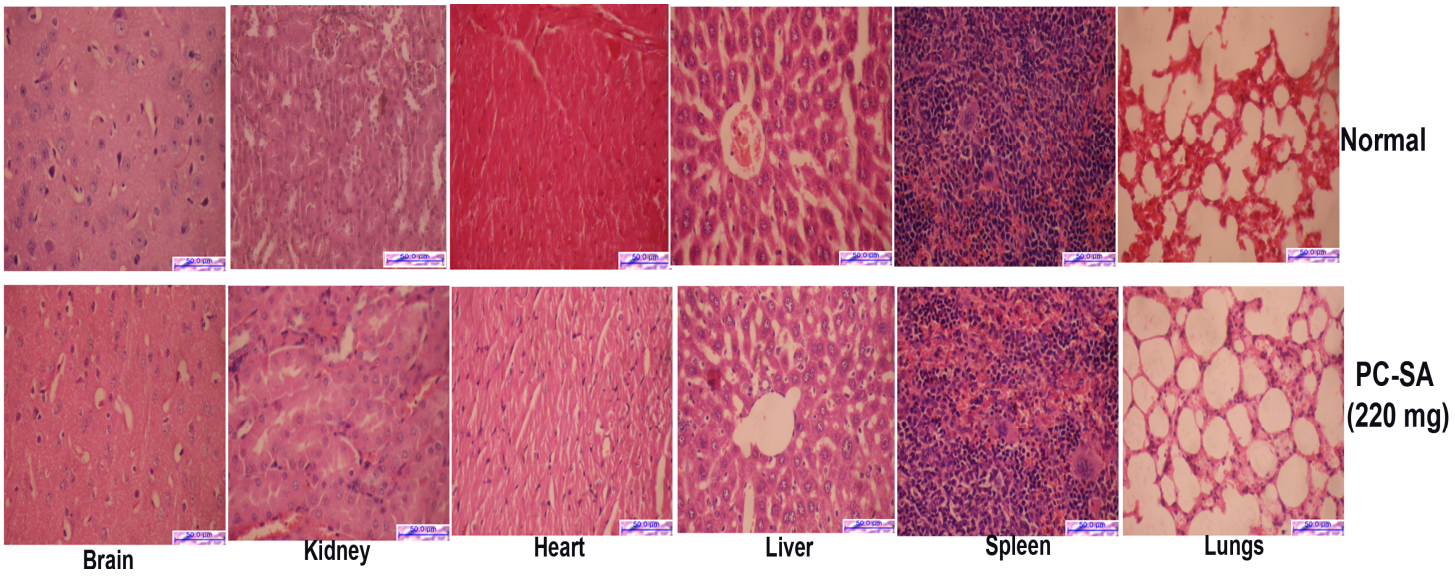

Figure S7: Acute toxicity study. Histopathology of vital organs (brain, kidney, heart, liver, spleen and lungs) in normal and 220 mg of PC-SA liposome treated (within 24 h) Swiss albino mice 15 days after i.v. administration. Scale bar 50 µm and magnification 40x.

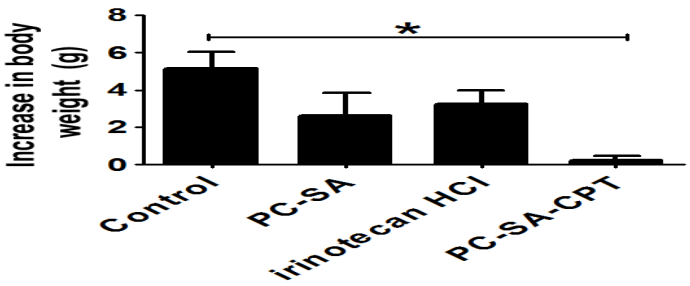

Figure S 8: No increase in body weight between day 0 and 21 of EAC innoculated Swiss albino mice treated with PC-SA-CPT. Mice were innoculated with EAC cells i.p on day 0 and on day 3. Mice were treated with 22 mg of PC-SA, 20 mg/kg body weight of irinotecan HCl and 20 mg/kg body weight of CPT entrapped in 22 mg of PC-SA. Body weights of the mice were recorded on day 0 and 21 and increase in body weights were calculated. All data represent the mean of triplicate experiments, with error bars indicating the s.e.m.

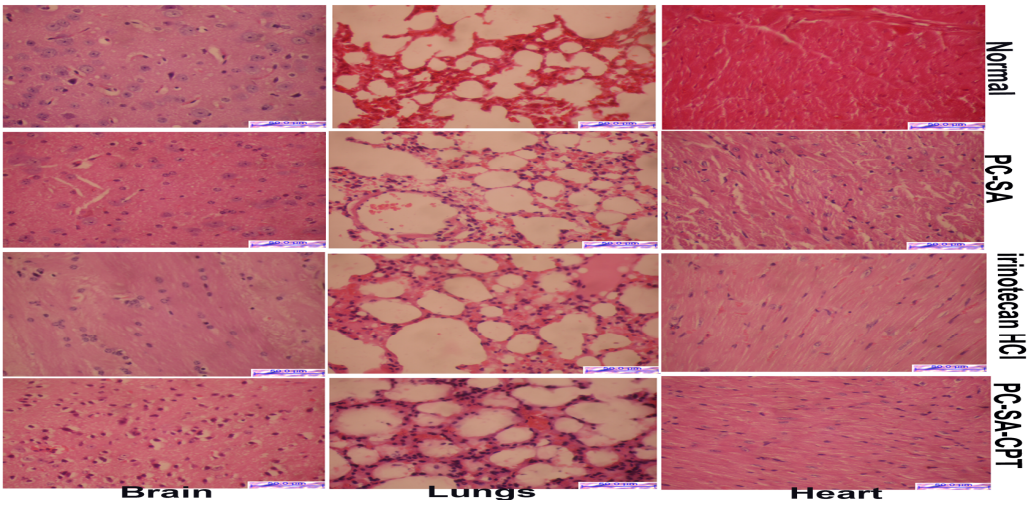

Figure S 9: Toxicity study of brain, lungs and heart in normal Swiss albino mice. Histopathological examinations of the tissues of brain, lungs and heart in normal, 22 mg PC-SA liposome, 20 mg/kg irinotecan HCl and 20 mg/kg CPT entrapped in 22 mg of PC-SA liposome treated Swiss albino mice 15 days after i.v. administration. Scale bar 50 μm and magnification 40x.

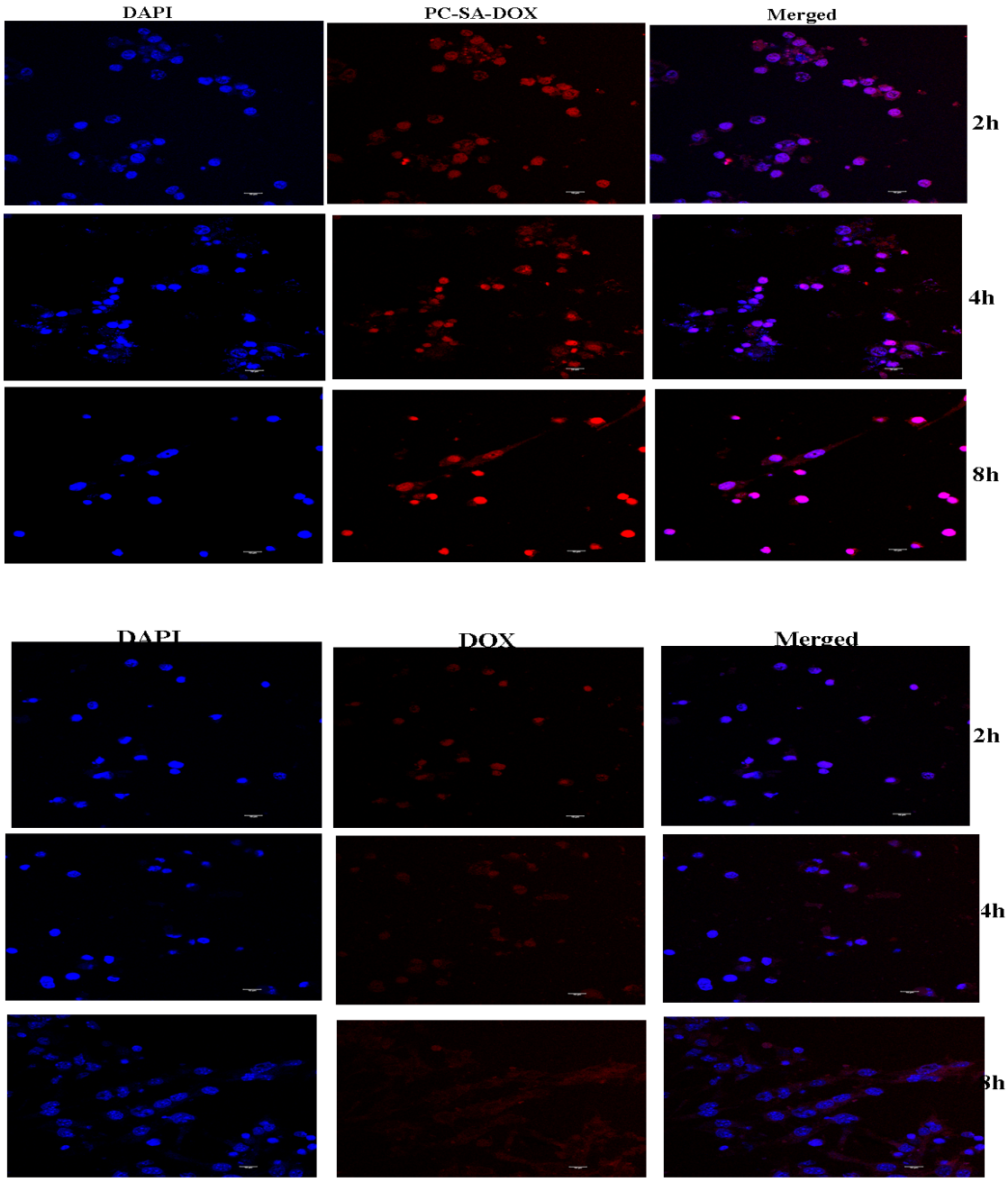

Figure S 10: Uptake of PC-SA-DOX and free DOX by B16F10 tumor cells: Confocal microscopy (Leica TCS SP8, software LAS-X) of B16F10 tumor cells taken out at 2, 4 and 8 h time points from B16F10 tumor induced C57BL6 mice injected s.c. with 4 mg/kg of free DOX or 4 mg/kg of DOX entrapped in 11 mg of PC-SA liposome. Scale bar 10 µm.

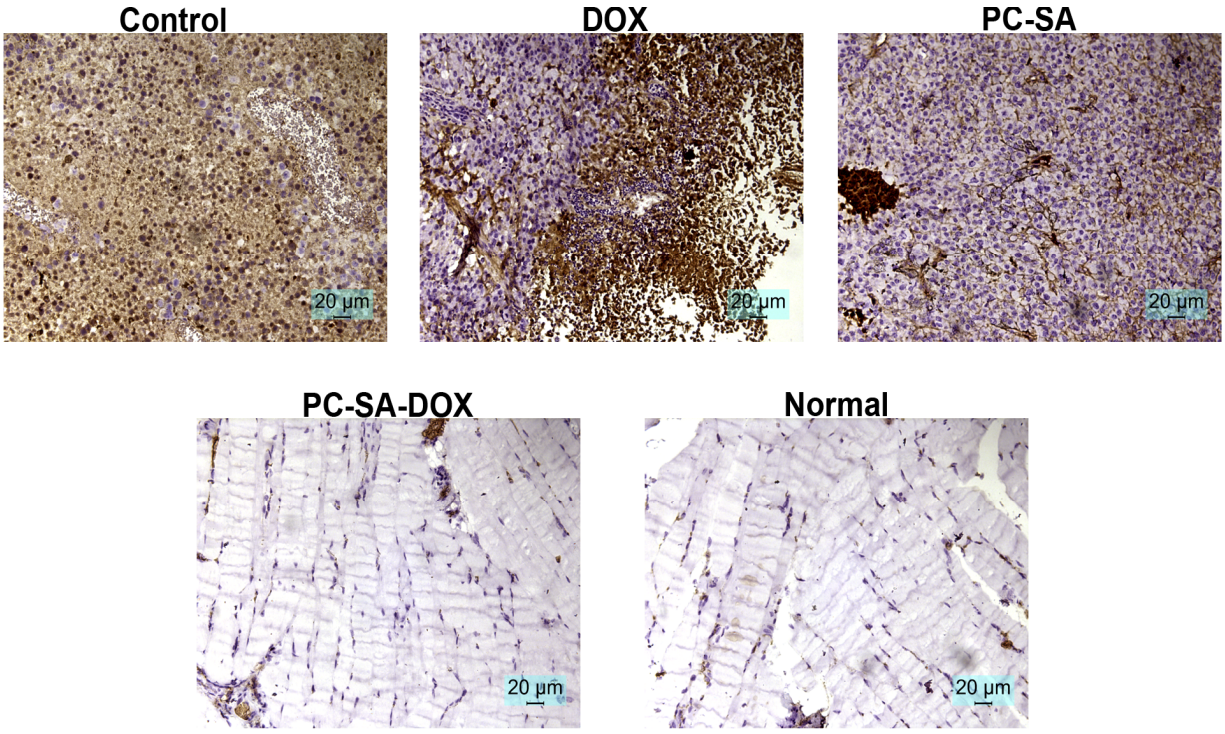

Figure S 11: Immunohistochemical analysis of tumor and normal tissue sections for expression of CD31 (marker used in vascular tumor). Tumor tissue sections obtained from B16F10 tumor induced C57BL6 mice treated on days 7 and 16 of tumor induction with 60 mg/kg of PC-SA, 2.8 mg/kg of DOX and 2.8 mg/kg of DOX entrapped in 60 mg/kg of PC-SA mice and normal tissue section underwent immunohistochemical analysis for the expression of CD31 and visualized under microscope (magnification, 40x, Scale bar: 20 µm).

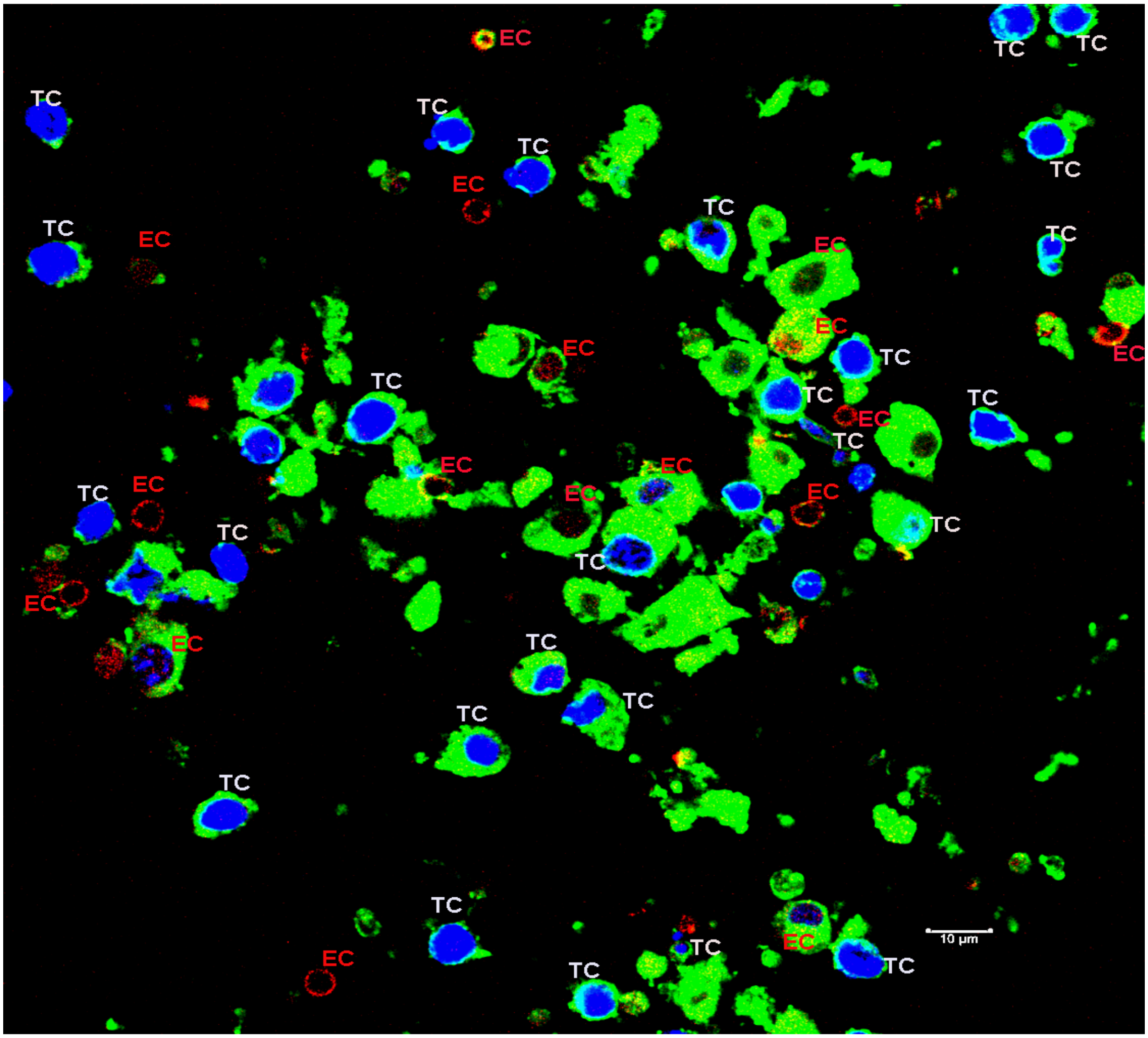

Figure S 12: Uptake of PC-SA liposome by endothelial cells and tumor cells: Confocal microscopy (Leica TCS SP8, software LAS-X) of endothelial cells (marked red EC) and tumor cells (marked TC) isolated from B16F10 tumor induced in C57BL6 mice and injected at the tumor site with PC-SA-FITC (green) liposome. Nuclei are stained with DAPI (blue). Scale bar: 10µm.

Supplementary Table 1

Time (hour)	**^{99m}Tc-PC-SA liposome Labelling Efficiency (%)**
1	**96.41 ± 0.18**
2	**95.53 ± 0.29**
3	**93.81 ± 0.34**
4	**90.66 ± 0.27**

Supplementary Table 1. Stability of ^{99m}Tc-PC-SA lipsome at room temperature at different time points, values represent mean ± Standard Error (SE) (n = 3).